DETECTION OF *BACILLUS* SPORES BY APATMER SELECTIVITY USING ATOMIC FORCE MICROSCOPY

THESIS

Nina M. Houtkooper, Captain, USAF

AFIT/GAP/ENP/05-03

DEPARTMENT OF THE AIR FORCE
AIR UNIVERSITY

AIR FORCE INSTITUTE OF TECHNOLOGY

Wright-Patterson Air Force Base, Ohio

DETECTION OF *BACILLUS* SPORES BY APTAMER SELECTIVITY USING
ATOMIC FORCE MICROSCOPY

THESIS

Presented to the Faculty

Department of Engineering Physics

Graduate School of Engineering and Management

Air Force Institute of Technology

Air University

Air Education and Training Command

in Partial Fulfillment of the Requirements for the

Degree of Master of Science (Applied Physics)
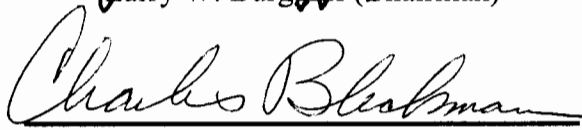
Nina M. Houtkooper, BS

Captain, USAF

June 2005

DETECTION OF *BACILLUS* SPORES BY APATMER SELECTIVITY USING
ATOMIC FORCE MICROSCOPY

Nina M. Houtkooper, BS
Captain, USAF

Approved:

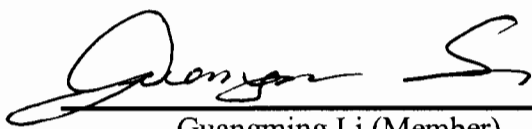_Larry W. Burggraf_

Larry W. Burggraf (Chairman)

19 May 2005

date

Charles Bleckman

Charles A. Bleckmann (Member)

19 May 05

date

Guangming Li

Guangming Li (Member)

8 May 05

date

AFIT/GAP/ENP/05-03

Abstract

The anthrax attack of Oct 2001 demonstrates the need for a rapid detector for spores of *Bacillus anthracis* (BA). Current technology requires cultures of BA to be grown for 24 hours. Using aptamers, a type of nucleic acid ligand selective for a target molecule, to select BA spores for measurement without culturing, is a possible solution for quicker detection. An aptamer having a specially selected structure is expected to selectively bind to the surface of its target spore, separating it from other material. An atomic force microscopy (AFM) method was developed to test this selectivity. Aptamers having structure selected to recognize BA were attached to a silicon nitride AFM probe, which was put in contact with spores of *Bacillus anthracis* Sterne strain or *B. thuringiensis* var. kurstaki (BT). Using the AFM in contact mode, the adhesion force between the aptamer and the spores was measured. This research compared the difference in adhesion forces of a clean probe and a probe treated with these aptamers for both BA spores and BT spores to determine whether the enhanced selectivity of aptamers for BA compared with BT could be directly measured.

Acknowledgments

I would like to thank my thesis advisor, Dr. Burggraf for his guidance, Dr. Bleckmann for his expertise in microbiology, and Dr. Li for his patience in teaching me how to use the atomic force microscope. I would also like to thank the folks at Air Force Research Laboratory, Counter-proliferation Branch. I am grateful for the instruction in the microbiology lab and with aptamers. Special thanks to Dr. Eric Holwitt, Amy Heathman, and Veronica Franz for sharing their expertise in microbiology and chemistry and their experience in the lab.

Nina M. Houtkooper

Table of Contents

List of Figures

List of Tables

DETECTION OF *BACILLUS* SPORES BY APTAMER SELECTIVITY USING
ATOMIC FORCE MICROSCOPY

I. INTRODUCTION

Biological agents have been around for thousands of years. During the 6th

Century B.C., the Assyrians poisoned enemy wells with a fungus that would make them

delusional (1). In the 14th Century siege of Kaffa, the Tartar force catapulted bodies of

plague victims into the city (2: 237). During Pontiac's Rebellion in 1763, the British

Army gave blankets infected with smallpox to the representatives of the Delaware

Indians (3). Recently, anthrax has been used as a biological weapon.

In October 2001, letters containing anthrax were sent to the several targets,

including the National Broadcasting Company, the American Broadcasting Company, the

Columbia Broadcasting Company, and U.S. Senator Tom Daschle (4: 593). The attack

caused several fatalities and thousands of people were put on a two month course of

antibiotics in an effort to preempt anthrax infections (5). This also caused the closure of

twelve senate offices and postal facilities in Washington D.C (4:593). The

decontamination of the Brentwood postal facility alone took 26 months and cost $130

million (6).

The low cost and ease of production and the possibly large amount of

contamination make biological agents great terrorist weapons (2: 235). *B. anthracis*

would be an ideal weapon for bioterrorism. As we saw in Oct 2001, the spores were very

hard to detect and contamination was easily spread. One deep breath of weaponized

aerosol anthrax spores (ID_{50} $8\cdot10^3 - 4\cdot10^4$) may contain as much as 10^5 spores (7: 337).

"The World Health Organization estimated that 50 kg of anthrax spores spread over a 2

km path of a city of 500,000 could result in 125,000 casualties and 95,000 deaths, making

anthrax the most formidable bioterrorism threat" (8: 324, 9: 171). An aerial spray of

anthrax spores along a 100 km line under ideal meteorological conditions could produce

50% lethality rates up to 160 km down wind (10: 552).

There are three modes to become infected with anthrax: cutaneous, which results

from spores infecting via skin abrasions; gastrointestinal, caused by ingestion of spore via

contaminated meat; and inhalational, resulting from inhalation of spores that have been

aerosolized (11: 46; 8: 324). Due to multiple methods of infection, there is a higher risk

for mass casualties.

The Centers for Disease Control and Prevention categorizes biological agents

based upon their risks for causing mass casualties in the event of a bioterrorist attack.

Bacillus anthracis was listed under Category A agents: "the highest priority, represent

organisms that (a) pose a risk to national security because they can be easily disseminated

or transmitted person-to-person; (b) cause high mortality, with potential for major public

health impact; (c) might cause public panic and social disruption; and (d) require special

action for public health preparedness" (9: 170). Due to the high priority the Centers for

Disease Control and Prevention has given spores of *B. anthracis*, a reliable means of

detection is required.

In response to the anthrax attack in 2001, a mobile laboratory was set up in the

Washington, D.C. area to conduct rapid molecular tests on collected environmental

samples (4: 593). The tests performed by the mobile laboratory required cultures to be

grown overnight (4: 594). With the ease of contamination, in a 24 hour time period many

more people could become infected. A method that does not require the growth of a

culture is needed. One possible method is the detection of spores with the aid of

aptamers. An aptamer would bind with the surface of the spore so no cultures would

have to be grown. This would reduce the detection time significantly.

Aptamers

Many advances have been made in the ability to produce a type of nucleic acid

ligand known as an aptamer, from the Latin 'aptus', meaning 'to fit' (12). Aptamers are

DNA or RNA molecules that have been selected from random pools of DNA or RNA

based on their ability to bind other molecules (13).

Systematic evolution of ligands by exponential enrichment (SELEX) (Appendix

A) is technique used to identify aptamers (14; 820; 15:810). The SELEX process screens

a large library of oligonucleotides by an iterative process of in vitro selection and

amplification (: 810). These functional nucleic acids can act as binding species

(aptamers) and catalytic nucleic acids (ribozymes and aptazymes.)" (: 810-811) The

SELEX process has been used to make aptamers that bind to a variety of targets ranging

from molecules to cells with high affinity and specificity (14: 820; 15: 810).

Current applications of aptamers include uses as detectors in medicine. With

advancing technology, different types of detectors are being explored including the use of

fluorescent labels and cantilevers. In each method, aptamers are allowed to bind to their

target molecule. The first method involves attaching aptamers of proteins associated with

cancer with a fluorescent label on the 3' end and attaching the 5' end to glass. Target

recognition is detected by a change in the fluorescent emission of the labels (16:245). The second method involves attaching the aptamer to a cantilever and allowing the cantilever to attach to its target molecule. The change in frequency of the cantilever denotes the detection of the target molecule (17: 3194; 18: 4490). Other cantilever works include works with the protein immunoglobin E aptamer using atomic force microscopy to measure the amount of force need to separate individual acceptor/ligand interactions (19: 2112, 2114). No *B. anthracis* aptamer work could be found. As work continues with building detectors, research is ongoing on understanding how the aptamer binds to its target molecule.

Each species of aptamer binds differently to its target molecule. "Many in vitro-selected aptamers adopt their final fold only after ligand binding, with the ligand being the essential part of the structure. In the absence of the ligand, the RNA is rather unstructured" (20: 104). The binding processes do have some commonalities.

An example of this is adenosine triphosphate (ATP) (Figure 1). Prior to binding with its aptamer shown in Figure 2, the purine-purine pairs are not stably formed (21: 12370). ATP recognition induces conformational change, stabilizing the molecule. Figure 3 illustrates the ATP aptamer bound to the ATP molecule. "Hydrogen bonds are clearly of great importance for the stability and specificity of the ATP-aptamer complex" (22: 473). Hydroxyl groups of the aptamer participate in hydrogen bonds with ATP (22: 473).
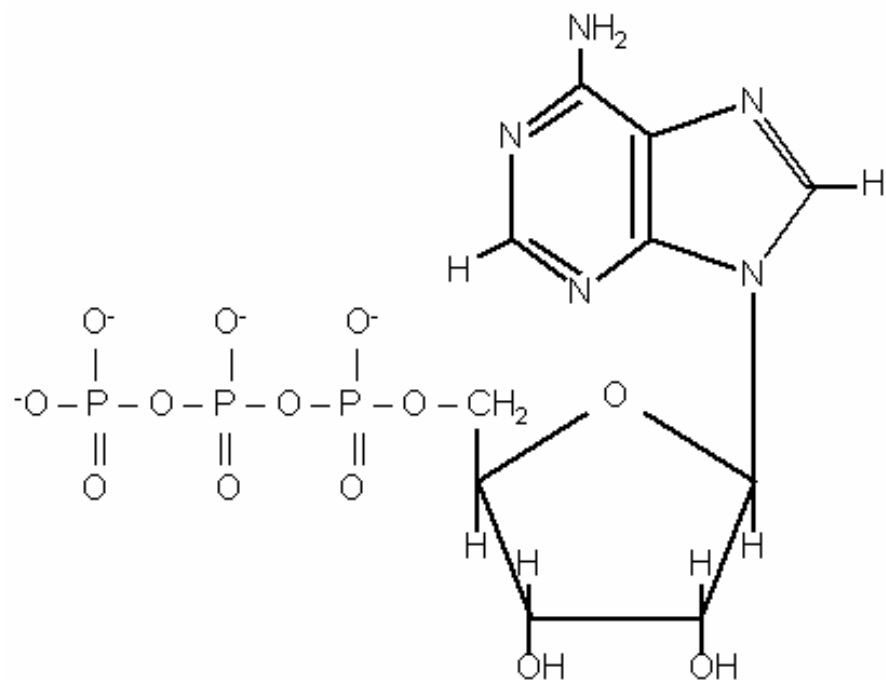
Figure 1. ATP molecule.
(23).
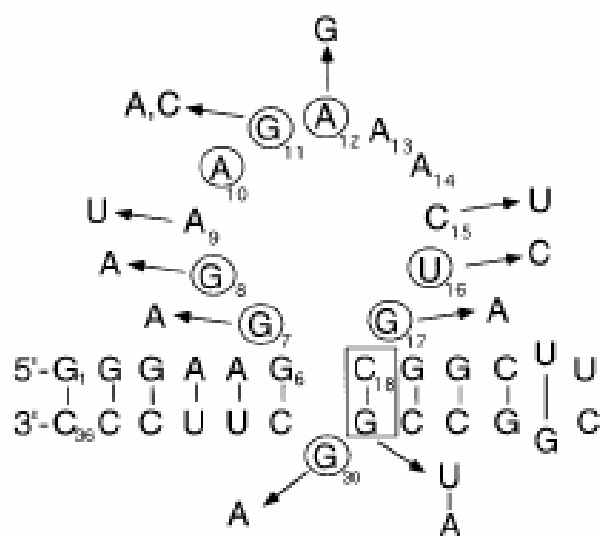
Figure 2. ATP binding aptamer.
(22: 468).
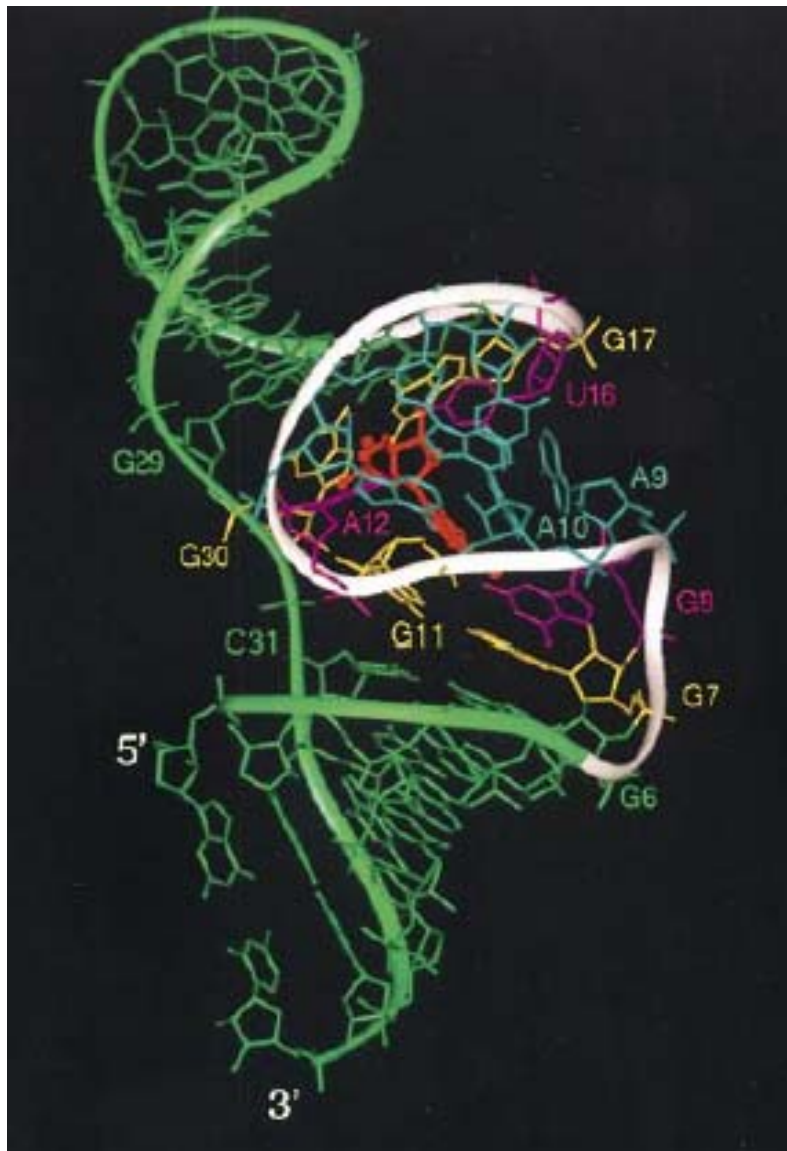
Figure 3. 3-D structure of ATP aptamer bound to ATP.
The ATP molecule is red (22: 468).

Like the ATP aptamer, the biotin aptamer (Figure 5) locks the biotin molecule

(Figure 4) into place by use of a hydrogen bond (24: 1238). "Extensive hydrogen

bonding by both the ribose and the base stabilize the nucleotide in this conformation"

(24: 1238).
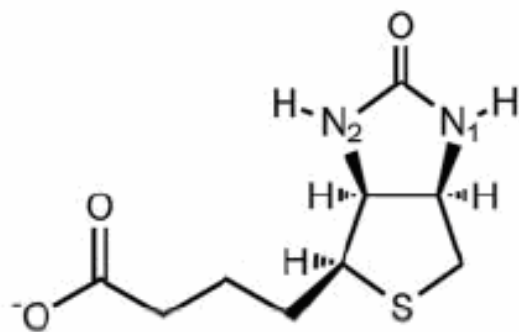
Figure 4. Biotin molecule.
(24:1236).
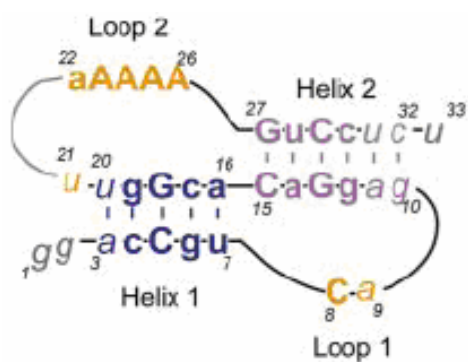
Figure 5. Biotin binding aptamer.
(24:1236).

Figure 6. Relative helical orientations of the biotin aptamer and biotin.
The biotin aptamer is in purple and the biotin molecule in green.
(24:1236).

In adenosine monophosphate (AMP), intermolecular hydrogen bonding and extensive stacking alignments of purine rings between AMP (Figure 7) and its aptamer (Figure 8) are associated with molecular recognition (25: 646).
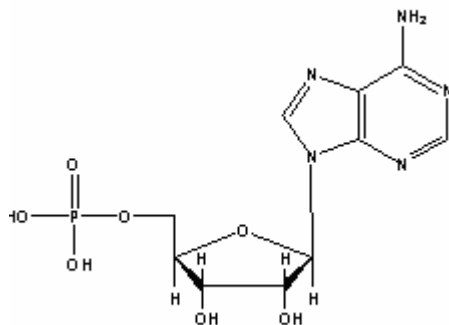
Figure 7. AMP molecule.
(26).
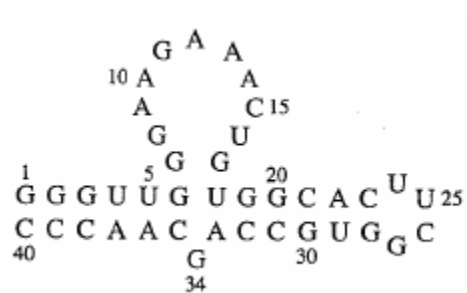
Figure 8. AMP binding aptamer.
(25:646).

Other molecules of interest are flavin mononucleotide (FMN) (Figure 9) and its aptamer (Figure 10). The formation of anti purine anti purine A8 G28 and G9 G27 mismatch pairs and the G10 U12 A25 base triple cause a widening at the FMN binding site, which facilitates the insertion of the isoalloxazine ring into the helix (25:651). "Binding specificity is associated with formation of two intermolecular hydrogen-bonds between the uracil like edge of the isoalloxazine ring and the Hoogsteen edge of anti A26

8

in the complex (25: 651). Figure 11 and Figure 12 show how the aptamer binds and is

stabilized by the aptamer.
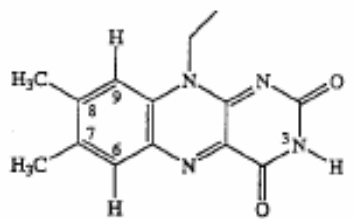
Figure 9. FMN molecule.
(25: 651).
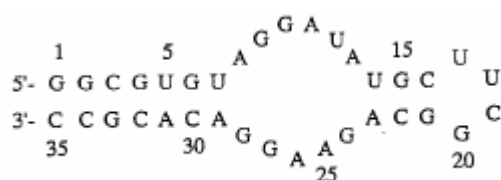
Figure 10. FMN binding aptamer.
(25:651).
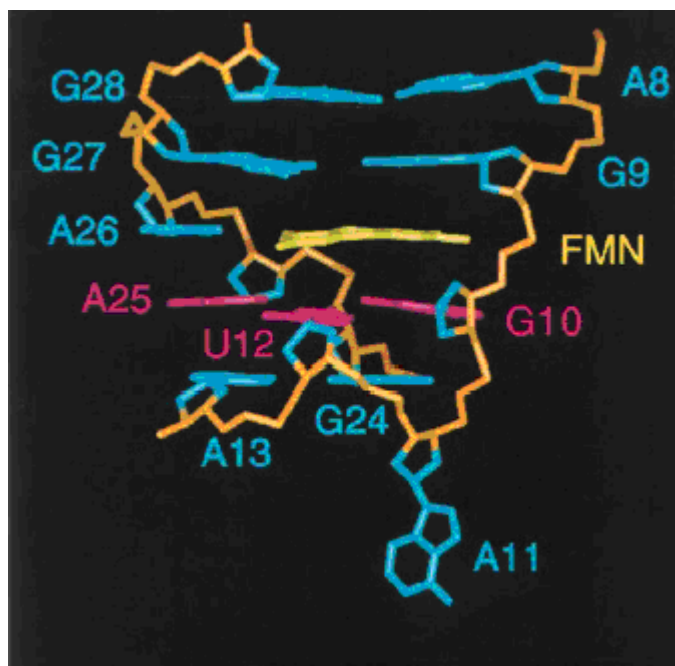
Figure 11. Model of FMN bound to aptamer.
View looking into the minor groove of the FMN bound
internal loop segment (A8 to A13 and G24 to G28) in the
complex (25:652).
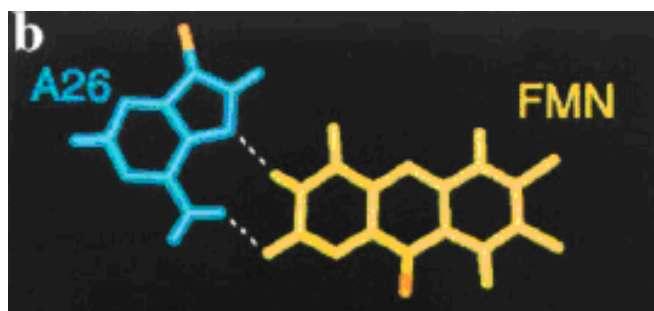
Figure 12. FMN stabilization by hydrogen bonds.
The A26 FMN alignment is stabilized by two hydrogen bonds involving the Hoogsteen edge of A26 (25:652).

The streptomycin binding aptamer (Figure 14) uses hydrogen bonds to recognize the streptomycin molecule (Figure 13). All of the NH_2, NH, and OH groups on the streptose ring are involved in intermolecular contacts while the two other streptomycin rings are outside the binding pocket, contributing only one hydrogen bond (20: 104). While aromatic ligands like ATP and FMN stack between bases, streptomycin lies perpendicular to the base pair planes (20: 104).
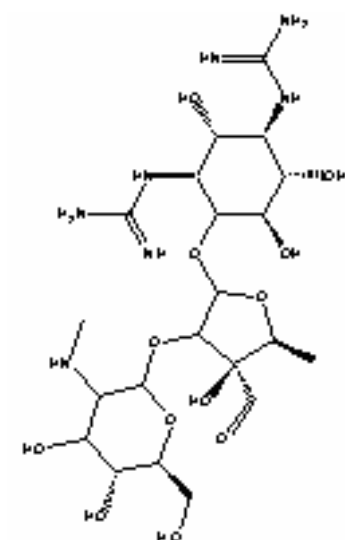
Figure 13. Streptomycin molecule.
(27).
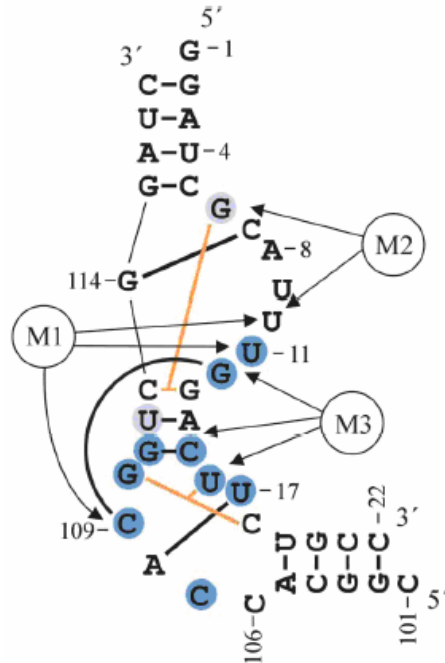
Figure 14. Streptomycin binding aptamer.
(20: 104).

As can be seen from the above examples, hydrogen-bonds play a key role in recognition and stability in the final conformation of the bound aptamer molecule. Purine-purine or other ring structure stacking also plays a key role in binding.

No literature was found on models of aptamers bound to *Bacillus* spores, but Figure 15 illustrates one possible conformation of the aptamer selective for *B. anthracis*. Like the aptamers mentioned earlier, this conformation has a loop structure that could play a key role in binding.

Figure 15. Proposed conformation of aptamer selective for *B. anthracis*.

11

The exact composition of the surface of the spore is still unknown, but there are molecules very similar to the ones mentioned above on the spore surface. This will be discussed in the next section.

Bacillus Spores

Bacillus are gram-positive, rod shaped, non-motile, spore forming, aerobic heterotrophs (28, 80; 29: 648). When a *Bacillus* bacterium enters its dormant state, it becomes a spore. This occurs when essential nutrients are exhausted. A single spore is produced within a vegetative cell and differs from it in increased resistance to adverse environments and absence of metabolic activity (30: 83). There are also major morphological changes described in Appendix B.

Structure

Bacillus spores vary by species, but have the same general structure (Figure 16). A core of DNA and enzymes is surrounded by layers of protective coatings (31: 14). The center of the spore is the spore core or protoplasm, which contains the nucleoid, enzymes, and ribosomes (: 16). Outside the forespore wall is the inner forespore membrane. After the inner forespore membrane is another thick layer of peptidoglycan is the spore wall (31: 16). This is located inside the cortex. "The spore wall will become the initial vegetative cell wall upon germination" (: 16). The cortex is composed of peptidoglycan, which helps cell walls keep their shape and is "thought to be essential for establishing relative dehydration in the central part of the spore (32; 31: 15). The forespore membrane surrounds the cortex. Outside the forespore membrane is a multilayered proteinaceous spore coat (31: 15). This coat aids in resistance to mechanical disruption,

chemicals, and enzymes (31: 15). The outer layer of coating is called the exosporium (31: 14).
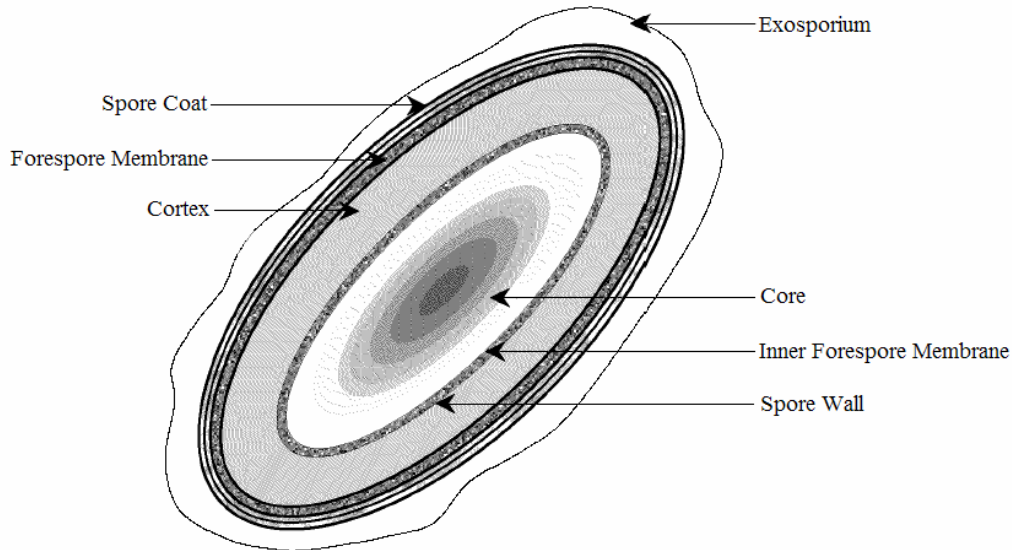
Figure 16. Structure of *Bacillus* spore.
(31: 14).

The exosporium consists of protein, polysaccharides, and lipids (33: 2). It is arguable that *B. anthracis*, and *B. thuringiensis* are the same species based on genes (34: 2627), but as similar as they may be, there are some difference that can be found in the exosporium Both *B. anthracis* and *B. thuringiensis* have galactose, galactosamine, rhamnose, and 3-*O*-methyl rhamnose, however Bt is distinct in that its exosporium also contains fucose and 2-*O*-methyl rhamnose (35: 146). As can be seen in Figure 17, all of these molecules have a ring structure, which as mentioned earlier, plays a key role in binding with aptamers. A certain configuration of these molecules will allow the aptamer to bind to the spore surface. This difference in exosporium composition might hold a key in the aptamers high selectivity for *B. anthracis* as opposed to *B. thuringiensis*.
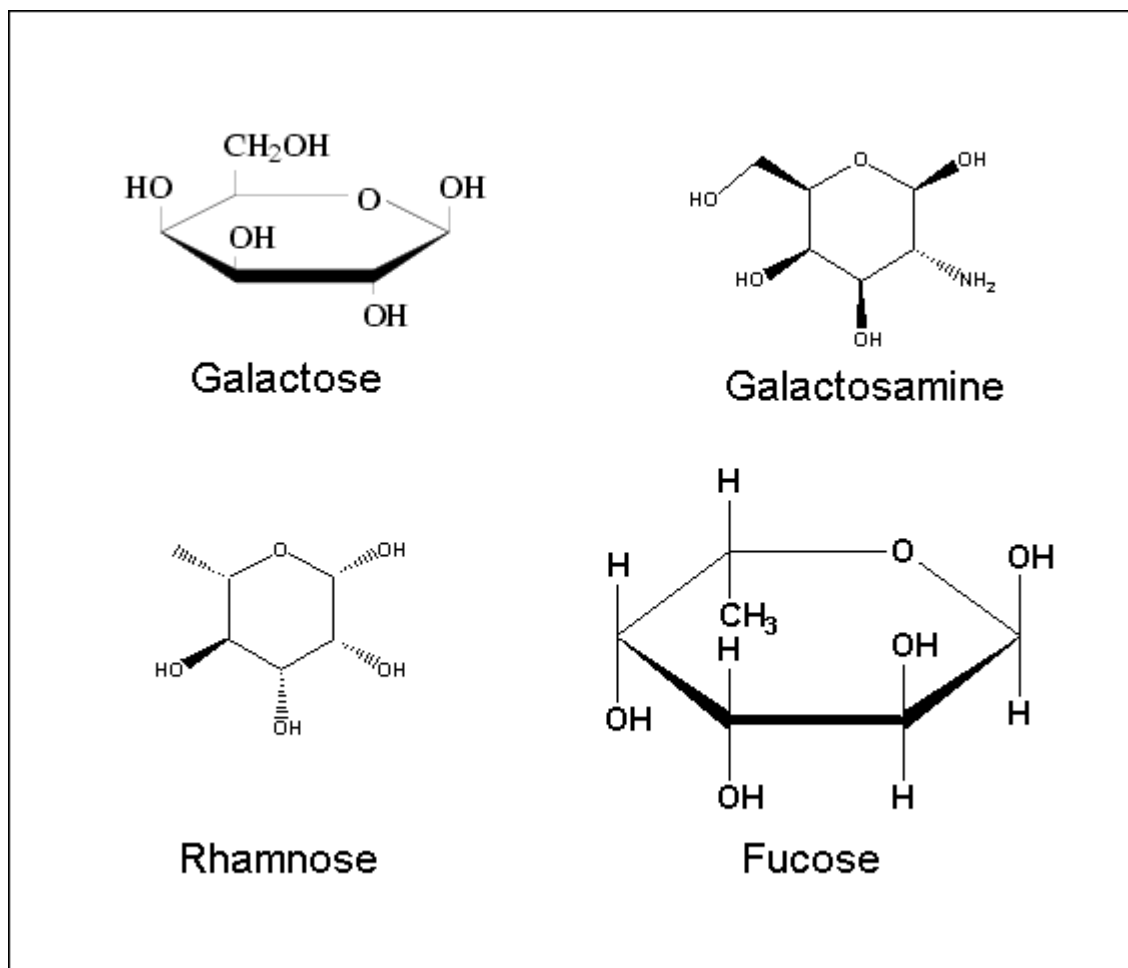
Figure 17. Molecules found in the exosporium.
(36).

Research is ongoing in this area. There are many proteins that have yet to be identified.

B. anthracis

B. anthracis, shown in Figure 18, is the causative agent of anthrax. When grown on blood agar, colonies form non hemolytic "Medusa head" shapes, or swirls with small tails sticking out (37: 323). The vegetative cells form little box car shapes attached end to end. Spores can be seen as little white dots when Gram stained.

Figure 18. Vegetative *B. anthracis*, gram stain, 1500x.
             B. anthracis cells (purple) are shaped like box cars. The
             endospores (white) are ellipsoidal shaped (38).

B. thuringiensis

The spores of *B. thuringiensis*, shown in Figure 19 are used as an insecticide often

spread from airplanes over fields (34: 2627). As can be seen in Figure 20, *B.*

thuringiensis produces a parasporal crystal protein, a protoxin which is responsible for

the fatal insect disease (39: 678). This crystal may also play a role in the aptamers of *B.*

anthracis ability to discriminate between the two species. Colonies are large with a small

hemolytic area and are prone to clumping.
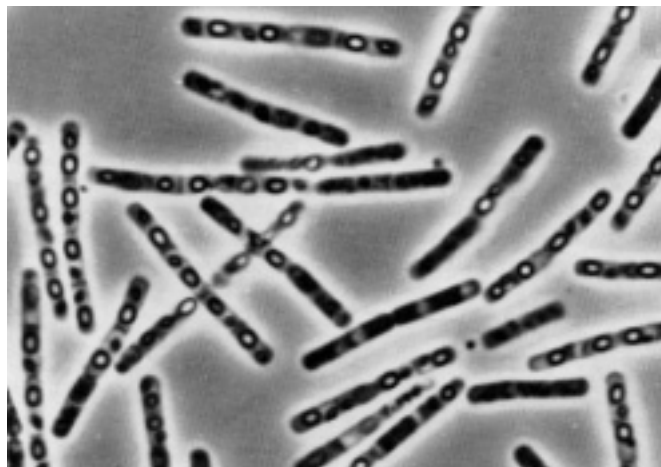
Figure 19. Phase photomicrograph of vegetative *B. thuringiensis* cells, 1000x.
             The intracellular spores are light colored and the parasporal crystals
             are dark (38).
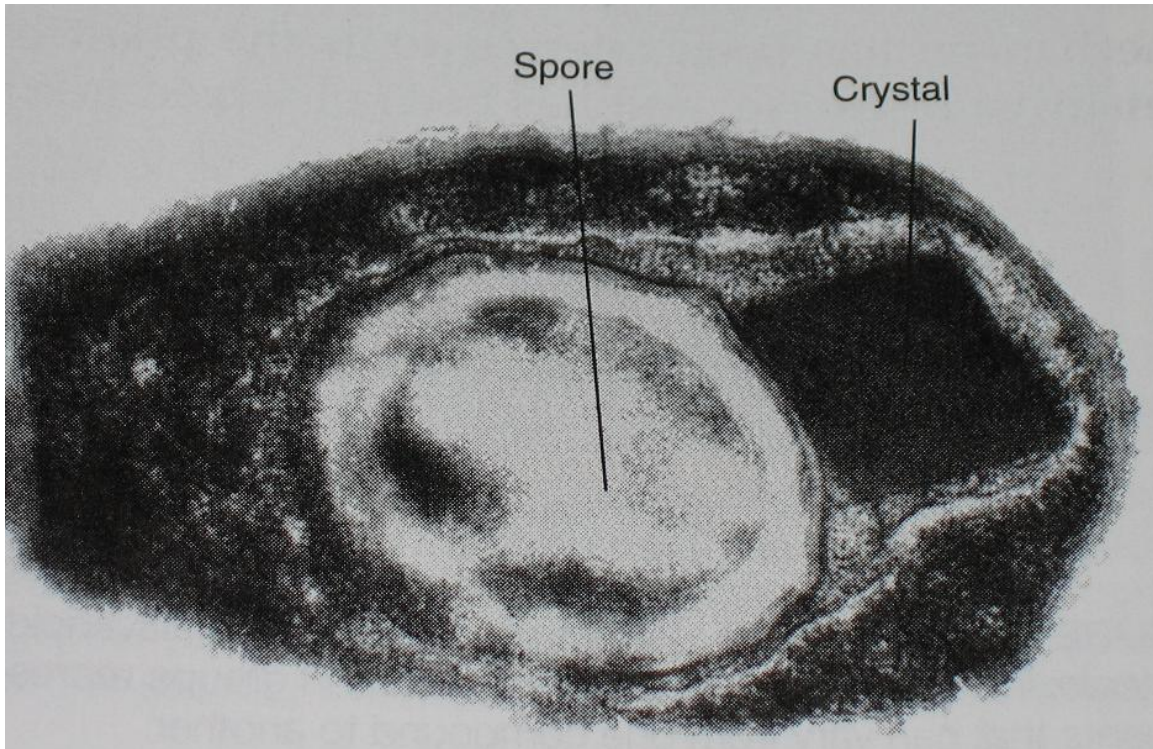
Figure 20. Electron micrograph of a thin section of the parasporal protein of *B. thuringiensis.*
(39: 678).

Atomic Force Microscopy

Atomic force microscopy acquires images with a minimum nanometer resolution utilizing a small probe by rastering a sharp tip across a surface, (40: 3655). An image is produced from the deflection of the cantilever as the probe scans across the surface (31:40).

Figure 21 shows a simplified model of how an atomic force microscope (AFM) works. Movement and position of the sample is controlled by the piezoelectric crystal. The laser (shown as red line) that monitors the probe is focused on the free end of the cantilever and the position of the beam is detected by a photodetector with a four element photodiode (41: 114). A computer records the three dimensional position of the probe and uses this information to generate an image of the surface (31:39).
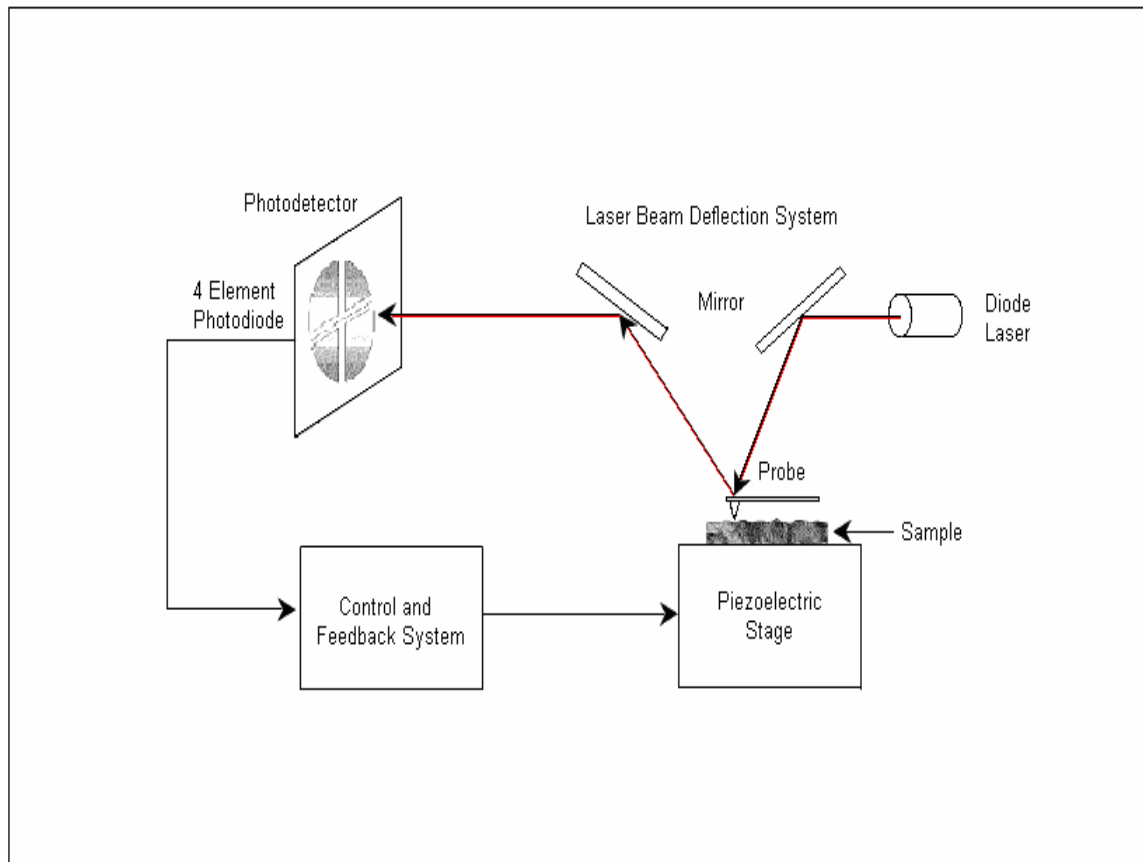
Figure 21. Overview of the atomic force microscope.
              The red line illustrates the path of the laser as it reflects off the
              mirrors and tip of the cantilever to the photodetector (31:40).

Contact mode has the capability of collecting height data, friction data, and force

data. Figure 22 is an AFM image of a *B. anthracis* spore. The image on the left is

generated from height data, taken from the cantilever moving up and down. The image

on the right is generated friction data, taken from the friction of the tip on the surface of

the spore as it scans across the surface. Force mode is a feature of contact mode that

allows for the measurement of the force applied on the surface from the tip. Figure 23 is

a force diagram in contact mode. This diagram shows the vertical deflection of the tip as

it moves across the surface. An explanation of this diagram can be found in Appendix C.

height data   friction data

4.75 µm 0   4.75 µm

Data type   Height   Data type   Friction
Z range   800.0 nm   Z range   1.000 V
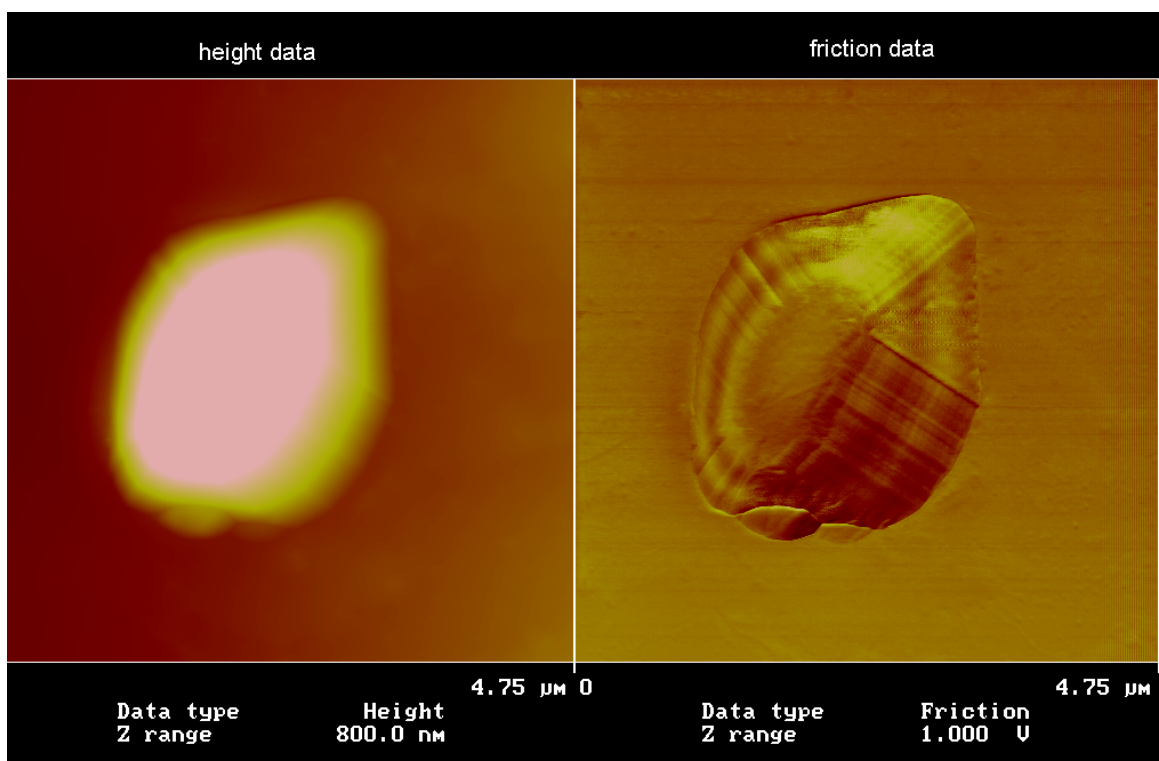
Figure 22. Contact mode AFM image of *B. anthracis* spore.
The image on the left is taken from height data and the image on the
right is taken from friction data.

Force Calibration Plot

⟵ Extending
⟶ Retracting

Deflection
79.50 nm/div

Setpoint

0.00   Z - 27.21 nm/div   544.25
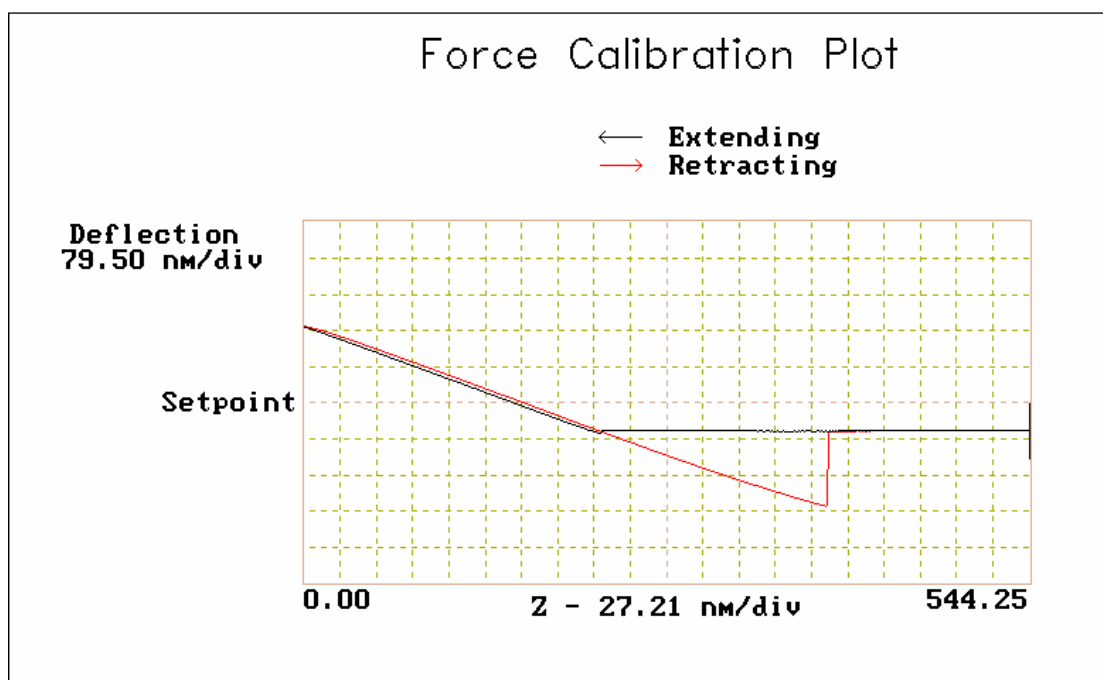
Figure 23. Contact mode AFM force diagram of *B. anthracis* spore.

II. Methodology

Experimental Overview

Aptamers selective for *Bacillus anthracis* Sterne strain attached to the tip of an AFM were put in contact with *B. anthracis* Sterne strain and *B. thuringiensis* variant *kurstaki* spores separately to test the ability of the aptamer to differentiate between spores. The two species of spores were grown and dropped onto a mica surface that was attached to a graphite wafer. The AFM was used in contact mode to measure the difference in force between a clean probe and a probe with aptamers selective for *B. anthracis* attached for both species of spores. These two species were chosen because they are very closely related genetically (31:1).

Force measurements were first taken using a clean probe on a 1 μm surface of the spore. The tip of the probe was then cleaned and dipped into an aptamer solution. Once dry, force measurements were taken and compared to the initial force with the clean tip. Blank measurements were also taken of the clean tip on a clean surface and the dipped tip on a clean surface.

Microorganisms

For this experiment, spores suspended in liquid were the easiest to handle.

Source

The original sample of *Bacillus* spores were provided to the Air Force Institute of Technology by Dr. Eric Holwitt of the Air Force Research Laboratory, Human Effectiveness Directorate, Counter-proliferation Branch, Brooks City Base, Texas in lyophilized form. The source of *B. anthracis* Sterne strain was a veterinary,

nonencapsulated, live culture of the anthrax vaccine (Thraxol-2 Code 235-23). The *B. thuringiensis* var. *kurstaki* was isolated by Brooks personnel from the insecticide Javelin® (Ortho® brand, no longer manufactured).

Growth

All sterilization was done in a Tuttnaur Brinkmann 3870 autoclave at 121 C and 15 psi for 15 minutes. The water used for this experiment was Millipore filtered deionized water (dH_2O).

Lyophilized *Bacillus* spores were used to create a liquid seed prep. A small amount of spores were poured into 150 mL of nutrient broth in an Erlenmeyer flask. The nutrient broth was prepared by mixing 4 g DIFCO Bacto Nutrient Broth and 500 mL of dH_2O, and then sterilized using the standard procedure mentioned above. The broth mixture was then incubated at 37°C and shaken for one day.

After incubation, an agar plate (Appendix D) was streaked with a sterilized wire loop dipped in the broth mixture. The streaked plate was incubated for one day at 37°C and stored in the refrigerator. To check for contamination, a colony was scraped from the streaked plate mixed with 1 drop of dH_2O on a slide. After the drop dried, the spores were heat fixed onto the slide by waving over the incinerator five times. The slide was then stained (Appendix E) using a Fisher Diagnostics Gram Stain Set (act. No. SG100D).

One day of incubation in the broth mixture allowed the bacteria to exhaust its nutrient supply, therefore 150 mL nutrient broth was added to the mixture. The seed prep was incubated and shaken for three days at 37°C. After three days, the bacteria had exhausted their nutrient supply. 13 mL of the seed prep was pipetted into six 15 mL centrifuge tubes and centrifuged for 20 min at 4°C and 4000 rpm. The supernatant was

poured off into a bleach solution and the pellet was resuspended in 2 mL of dH_2O. The six tubes were then vortexed for 5 seconds and combined into two tubes by pouring two tubes into one. The spore solution was then refrigerated at 4°C for three to five days. After refrigeration, the spore solution was heat shocked by putting the tubes in a 65ºC hot water bath for 30 minutes, after which the spores were ready to use. The spore solutions were stored in a refrigerator.

In order to make a super concentrated solution, a plate was streaked with the spore solution and allowed to incubate until the plate was covered with *Bacillus* and they had sporulated. The spores were then scraped off with a sterile loop and suspended in 3 mL of dH_2O. This solution was placed in the ultrasonic bath for 3 minutes. The purpose of the ultrasonic bath was to remove any vegetative debris still be attached to the spores. Seven mL of dH_2O was then added to the solution and it was centrifuged for 15 minutes at 3000 rpm and 4°C. The supernatant was poured off, the pellet was resuspended in 10 mL of dH_2O, and the solution was centrifuged again. This was repeated three times, with the addition of 3 mL of dH_2O instead of 10 mL at the end of the third repetition. Only 3 mL of dH_2O was added to the pellet to keep a high concentration for the sample. The samples were stored in the refrigerator at 4°C until use.

Spore Count

A dilution series and spore count (Appendix F) was run on the final spore sample to approximate the number of spores per mL. The plate was held under a light and magnifying glass to count the number of colonies grown. The following equation was used to calculate the colony forming units per mL:

21

$$\frac{number\ of\ colonies}{(dilution\ factor) \times (0.1\ mL)} \qquad (1)$$

where the dilution factor is the dilution number written on the test tube.

Aptamer Preparation

The *B. anthracis* aptamer was created by the Air Force Research Laboratory, Human Effectiveness Directorate, Counter-proliferation Branch, Brooks City Base, Texas, using the SELEX method described in Appendix A. The result of their work was a strand of 40 nucleotides that could be manufactured. The following sequence was ordered from Sigma Genosys: AGA GGA ATG TAT AAG GAT GTT CCG GGC GTG TGG GTA AGT C - C12 spacer - amine, with two different purification methods: PolyAcrylamide Gel Electrophoresis (PAGE) and High Performance Liquid Chromatography (HPLC). PAGE guaranteed to have 95 to 98% purity, while HPLC had a 90 to 97% purity guarantee. The 3' end of this sequence was modified with a 12 carbon chain followed by an amine. This was done for possible future experiment that may involve silation. The PAGE yielded 17.9 nmol and the HPLC yielded 26.1 nmol. 0.5 mL dH$_2$O was added to the 26.1 nmol sample.

Sample Preparation

For both the *B. anthracis* and *B. thuringiensis* solutions, 5 µL of the sample was dropped onto a clean sheet of mica attached to a graphite wafer, and allowed to dry under the hood. Samples were stored in a Petri dish. The *B. anthracis* sample was stored on the lab bench for 14 days prior to use. The *B. thuringiensis* sample was stored in a desicator for 7 days before use. For each sample, the mica was cleaned by applying

Scotch tape and removing it. The Scotch tape removed a layer of mica, exposing a clean

surface. For the dipping solution, 20 μL of aptamer solution was dropped onto a clean

sheet of mica attached to a graphite wafer and stored in a plastic Petri dish while not in

use. This was done daily.

Atomic Force Microscopy

The force mode feature of contact mode was used for the collection of all data.

Microscope Configuration

All images were taken using the Nanoscope® IIIa Scanning Probe Microscope

(Figure 24). The AFM was placed on a twenty pound granite base which was supported

by four isolation pads designed to dampen vibration during scanning. This was set up on

a vibration isolation table to further help with the damping. To aid with the viewing of

the sample area, the Nanoscope® Optical Viewing System was used. The optical camera

was mounted on top of the AFM, where it allowed the operator to view the sample

through an aperture at the top of the AFM head.
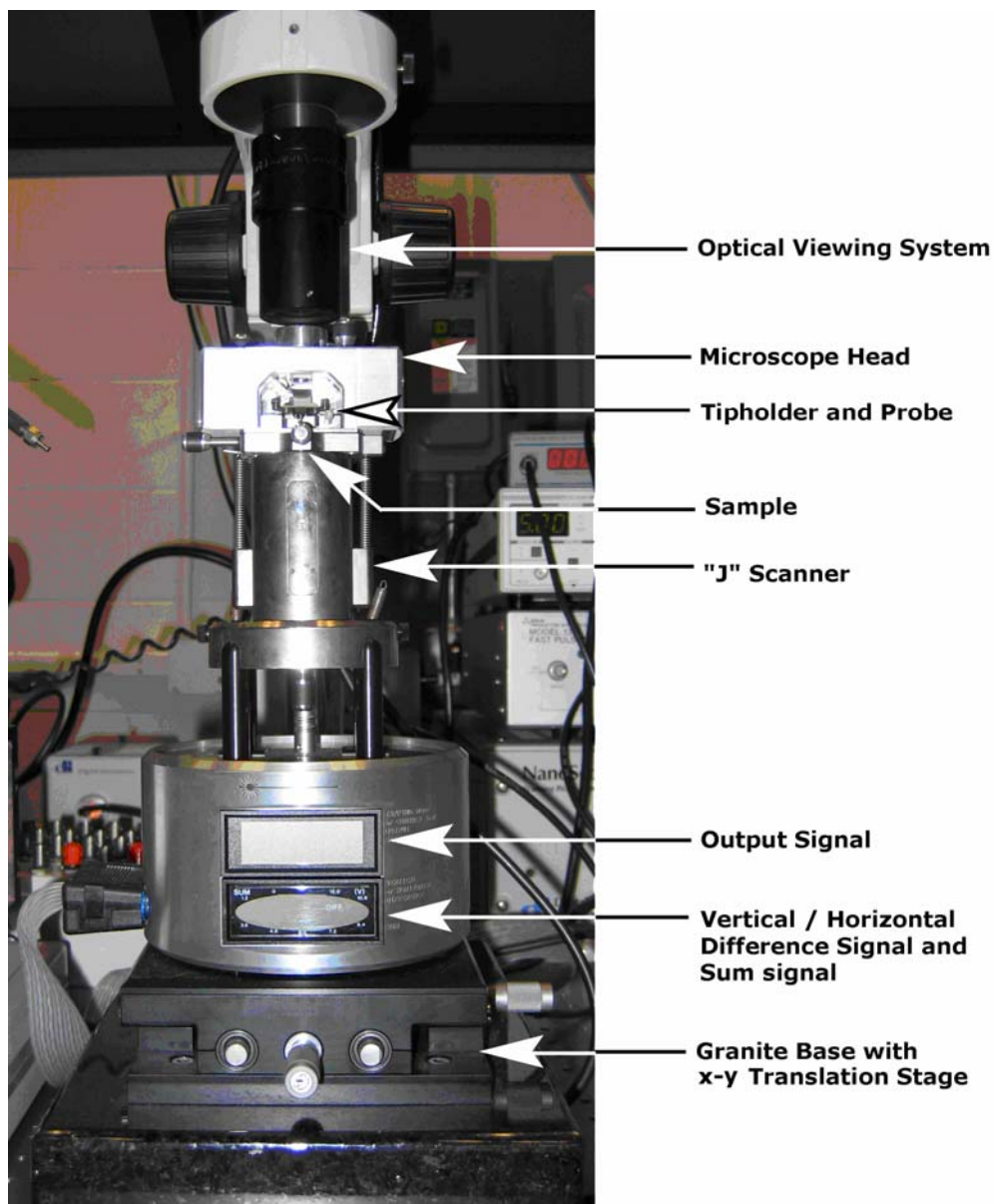
Figure 24. Nanoscope® IIIa Scanning Probe Microscope.

Preparation

After the sample was prepared on mica, it was inserted into the viewing area of

the AFM with tweezers. A magnet helped hold the sample in place on the stage. The

optical camera was focused such that the spores appeared as little black dots. A probe

was placed in the probe holder with the 0.58 N/m cantilever available for use. The tip

was aligned with the target spore and lowered until it was just above the surface of the sample.

The laser was then turned on in contact mode (a red light will show on the front of the AFM) and aligned with the tip to get a maximum SUM signal. Once the sum signal was maximized, the "Vertical or Horizontal Difference Signal" was adjusted to zero and the "Output Signal was adjusted to -2.0 volts. The deflection setpoint was set to 0.0 volts. Integral gain was set to 2.0 and proportional gain was set to 3.0 for the experiment. The scan frequency was set to 5.09 Hz. Once the initial adjustments of the AFM were complete, no adjustments were made. The tip was then engaged and lowered to the surface of the sample so the image could be taken.

Data Collection

Once a target spore was found, the spore was imaged at 1.0 μm. The tip velocity was set to 5.09 μm/s. (This value should be preset at 1.0 μm with the 5.09 Hz scan frequency set earlier.) The force mode feature of contact mode was enabled to collect force data at one point. Before capturing the force diagram, the deflection setpoint was calibrated by following the slope of the line where the piezo is retracting (points 3 through 5 of Figure 47). This was repeated two more times at various points as the tips scanned along the surface. Figure 25 shows an example of approximately where the force samples were taken. After the three force data points were collected on the spore, three blank data points were collected on a clean mica surface located on the sample. The optical camera was used to find a location with no spores. The tip was reengaged at 1 μm and three force data points were taken. The force data was first collected using a clean tip and repeated with a tip dipped in aptamer solution.
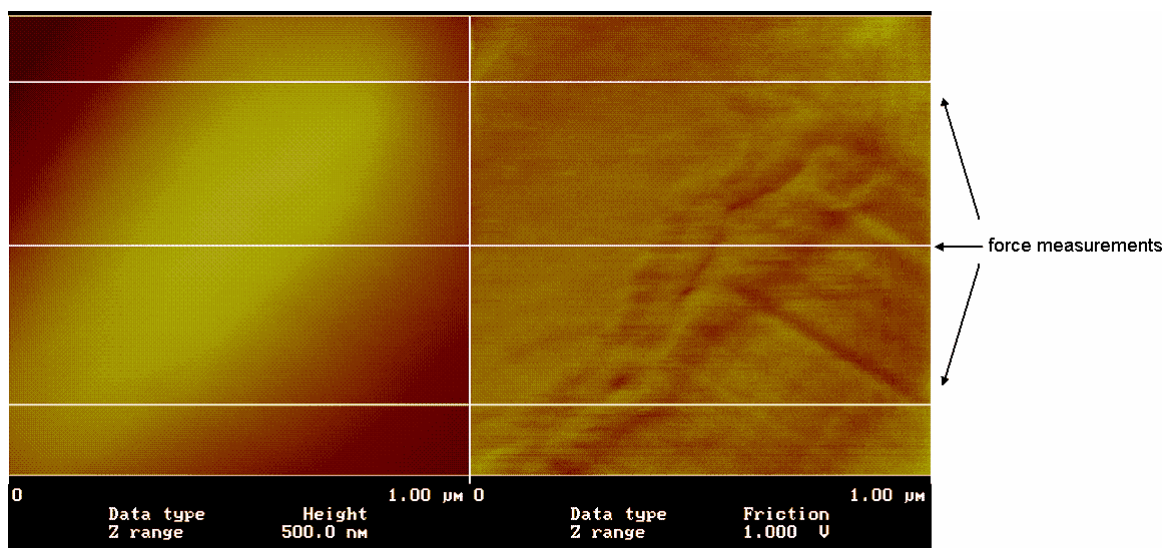
Figure 25. AFM image (contact mode) showing approximately where force
measurements were taken across the surface of a *Bacillus anthracis*
spore.

Once the data with the clean tip was collected, the tip was disengaged and

removed. To attach the aptamer to the tip of the cantilever, the tip was first cleaned by

rinsing with acetone and allowed to air dry. The aptamer dipping solution described

earlier was then placed in the viewing stage. The dried tip was then set in the probe

holder. The optical camera was focused on the surface of the sample and the tip was

lowered until it touched the surface. The tip was then raised and removed to dry. Once it

had dried, the tip was replaced and force data was collected on a spore and a blank as

described for the clean tip.

III. Results and Analysis

Overview

      For each tip used, force measurements were taken with a clean tip and a tip with aptamers attached (aptamer tip). The difference in force between the clean tip and the aptamer tip required multiple calculations, which can be found in Appendix H for *B. anthracis* and Appendix I for *B. thuringiensis*.

Calculations

      The difference in force between the aptamer tip and the clean tip is described by Hooke's law:

$$F = -k\Delta z \qquad\qquad (2)$$

where k is the spring constant of the cantilever, 0.58 N/m, and Δz is the displacement of the tip as it continues its scan, moving away from the spore. Figure 26 is a force diagram illustrating the difference in the initial displacement of the tip on the spore (blue line) and the release of the tip from the surface of the spore (green line) of each data point. To calculate Δz, the number of squares between the green and blue lines are counted and multiplied by the deflection setpoint.
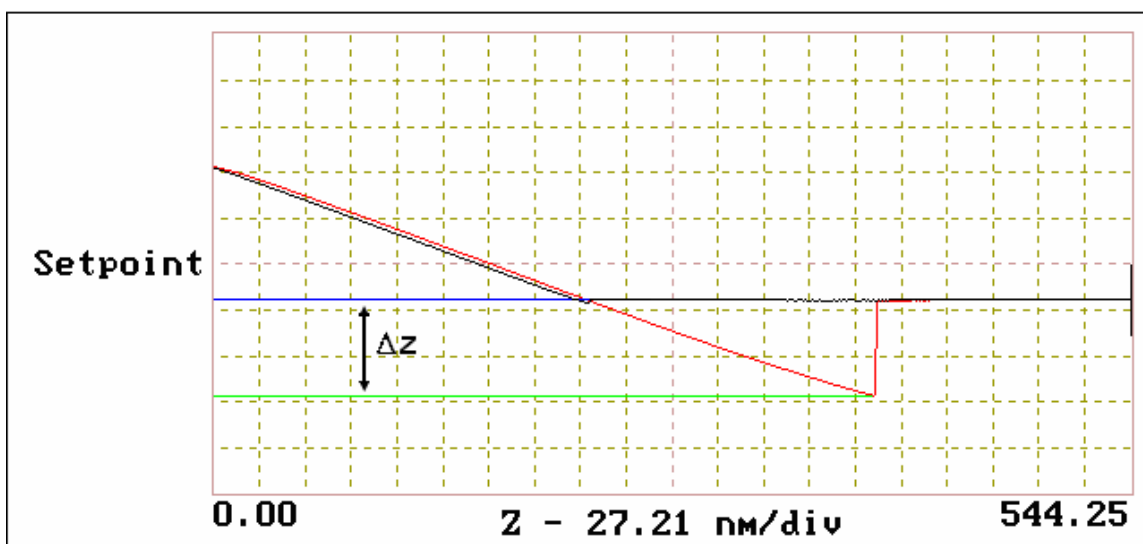
Figure 26. Force diagram showing measurement of Δz.

The force was calculated for each data point. An average was taken for the three points of each type of tip and surface (clean tip on the spore, blank clean tip, etc.). The difference in force was calculated using these averages.

Results for *B. anthracis*

The data in Appendix H is presented in graphical form in the next three sections. It is presented several different ways: basic force measurements, clean tip vs. aptamer tip interacting with a *B. anthracis* spore surface, clean tip interacting with a *B. anthracis* spore surface vs. clean tip interacting with a blank surface, and aptamer tip interacting with a *B. anthracis* spore surface vs. clean tip interacting with a blank surface.

Force Measurements

Figure 27 is a graph representing all of the force measurements taken for *B. anthracis*. There was no method available to determine the number of aptamers on the tip. If the aptamer tip force measurement appeared less than the clean tip force

28

measurement, the tip dipping procedure was repeated. This is the reason there are more data points for aptamer tips than clean and blank tips. Also, force measurements were captured, but the software did not save several force measurements correctly. (Force calibration plots showed a flat line with no interaction with the sample.) The data points were arranged from least to greatest force not to show a trend, but to illustrate the range of force measurements.
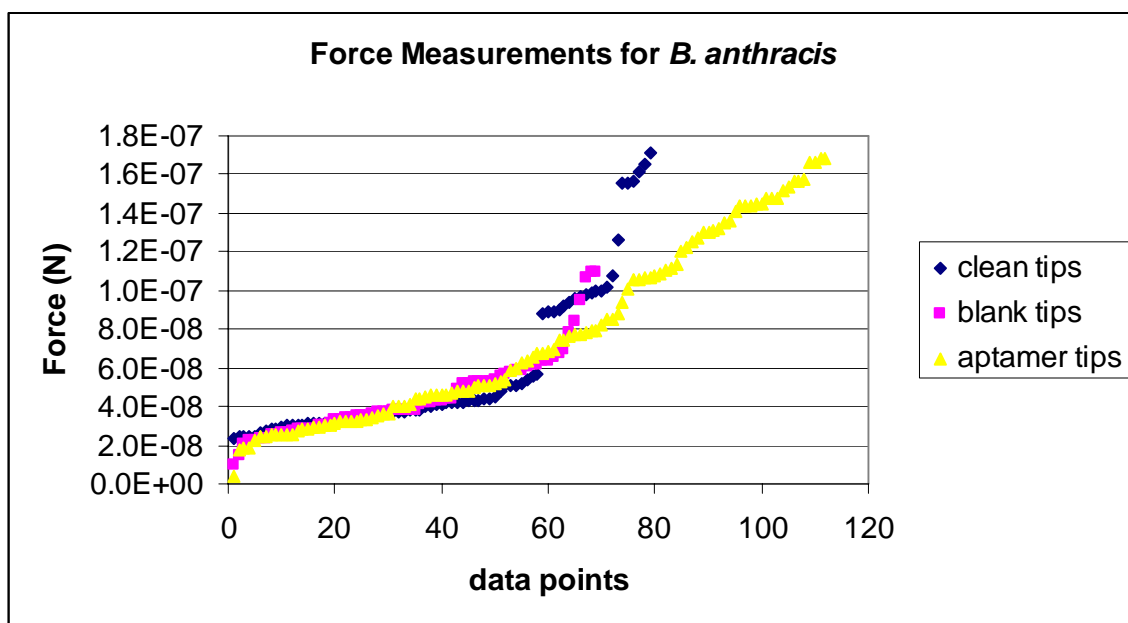
Figure 27. Graph of all force measurements for *B. anthracis.*

Figure 28 is a graph representing all of the data collected for *B. thuringiensis*. The tip dipping procedure was not repeated for these measurements so there are about the same number of measurements for each tip. The data points were arranged in order of least to greatest force not to show a trend, but to illustrate the range of forces.

Table 1 shows the statistics for all of the force measurements taken. In both the *B. anthracis* and *B. thuringiensis* measurements, the clean tips had the largest range (and standard deviation) and the blank tips had the smallest range (and standard deviation).

The number of aptamers attached to the tip is a possible explanation for the higher range of the aptamer tip force measurements.
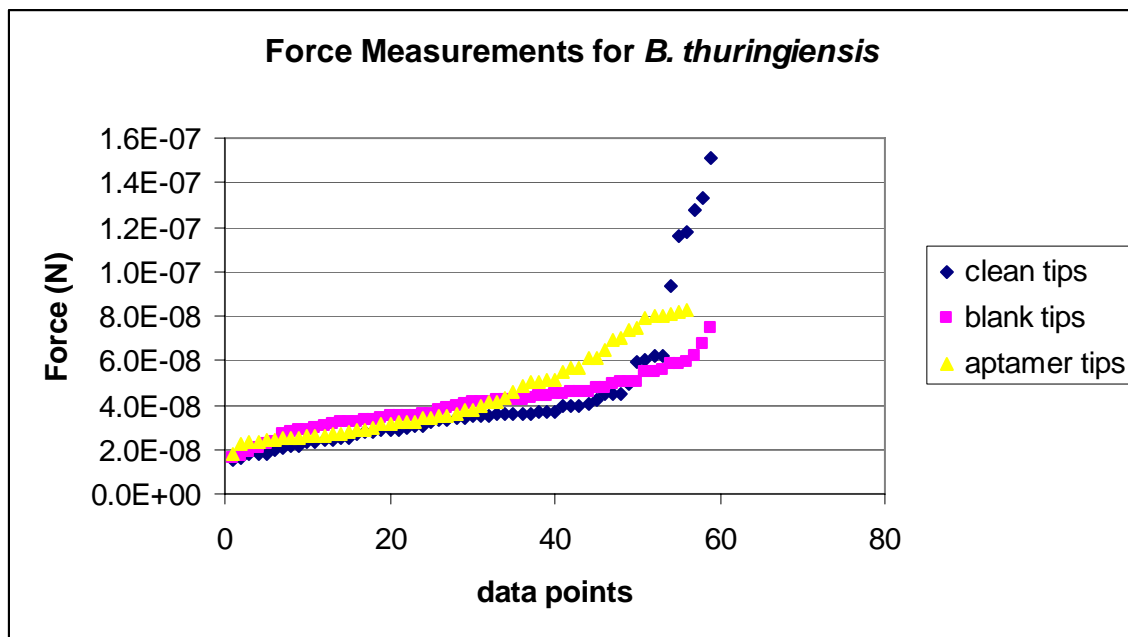
Figure 28. Graph of all force measurements for *B. thuringiensis.*

Table 1. Statistics for force measurement data.

| | Force (N) | | | | | |
| | B. anthracis | | | B. thuringiensis | | |
	clean tips	blank tips	aptamer tips	clean tips	blank tips	aptamer tips
Average	5.802E-08	4.571E-08	7.690E-08	4.245E-08	4.038E-08	4.390E-08
Standard Deviation	3.892E-08	2.134E-08	4.632E-08	2.995E-08	1.219E-08	1.918E-08
Range	1.480E-07	9.998E-08	1.638E-07	1.362E-07	5.799E-08	6.468E-08
Minimum	2.338E-08	9.636E-09	4.307E-09	1.513E-08	1.640E-08	1.829E-08
Maximum	1.714E-07	1.096E-07	1.681E-07	1.513E-07	7.439E-08	8.297E-08

The data points were averaged for each tip by type of measurement (clean tip, blank tip, etc.) and are presented in the next sections.

Clean Tip vs. Aptamer Tip Interacting with a B. anthracis ***Spore Surface***

Figure 29 represents the difference in force between the clean tip and the aptamer tip interacting with a *B. anthracis* spore surface. The negative measurements indicate

that the spore adhesion force was greater with a clean tip than an aptamer tip. As mentioned earlier, there was no method available to check the number of aptamers attached to the tip. Some failed tips were cleaned and dipped in the aptamer solution a second time, resulting in a positive difference in force.
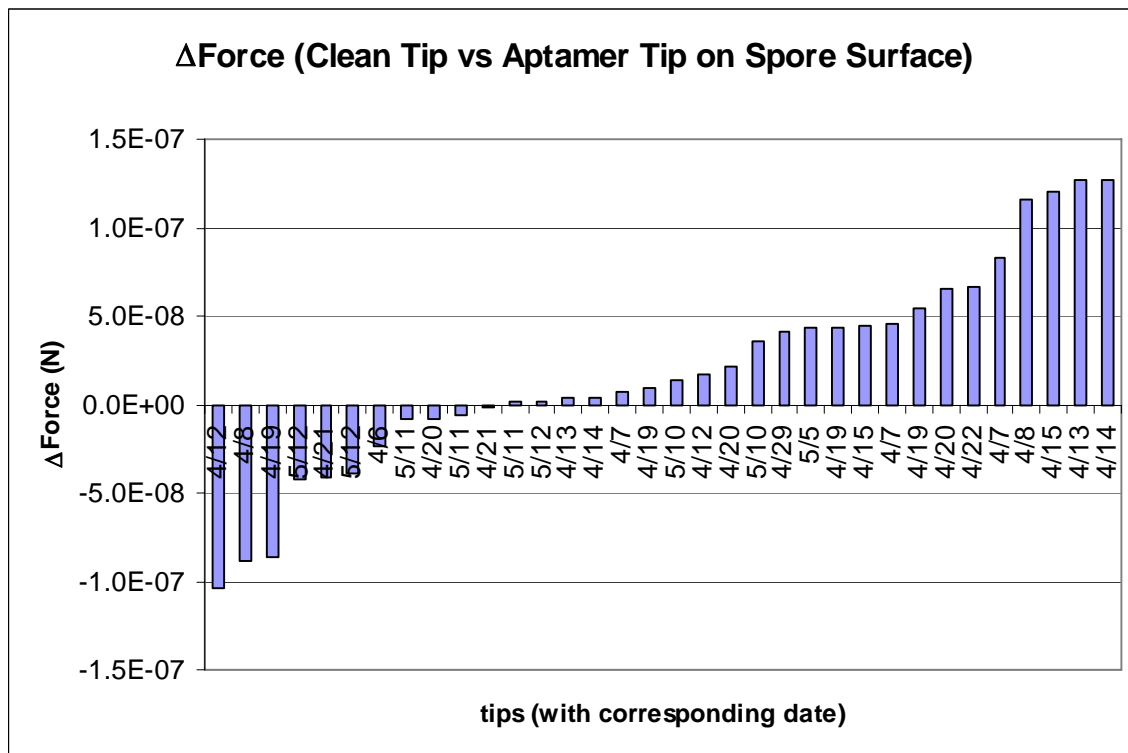
Figure 29. Graph of difference in force between clean tip and aptamer tip
interacting with *B. anthracis* spore surfaces.
The date was added on the x-axis to show that was no correlation
between the day the data was taken and the adhesion force.

The areas where the forces are equal could be from various factors. The number of aptamers attached to the tip could vary the adhesion force, since more force would be needed to break extra bonds between the aptamer and the spore. The radius of the tip in contact with the surface is about 6nm, which allows for the attachment of 2 to 4 aptamers to the tip.

Another factor is the humidity of the room. Bowers, et al, has been showed that at 64% relative humidity, adhesion force is reasonably reproducible, but at 33% relative humidity, there is greater variability with values below and above those at higher humidity (42: 208-209). A third factor would be the degree of hydration of the spore surface.

Figure 30 is a histogram representing the data from Figure 29. The areas that leveled out in Figure 29 can be seen as three peaks. This could be possible adhesion forces for the attachment of various numbers of aptamers the tip.

Histogram (Clean Tip vs Aptamer Tip on Spore Surface)
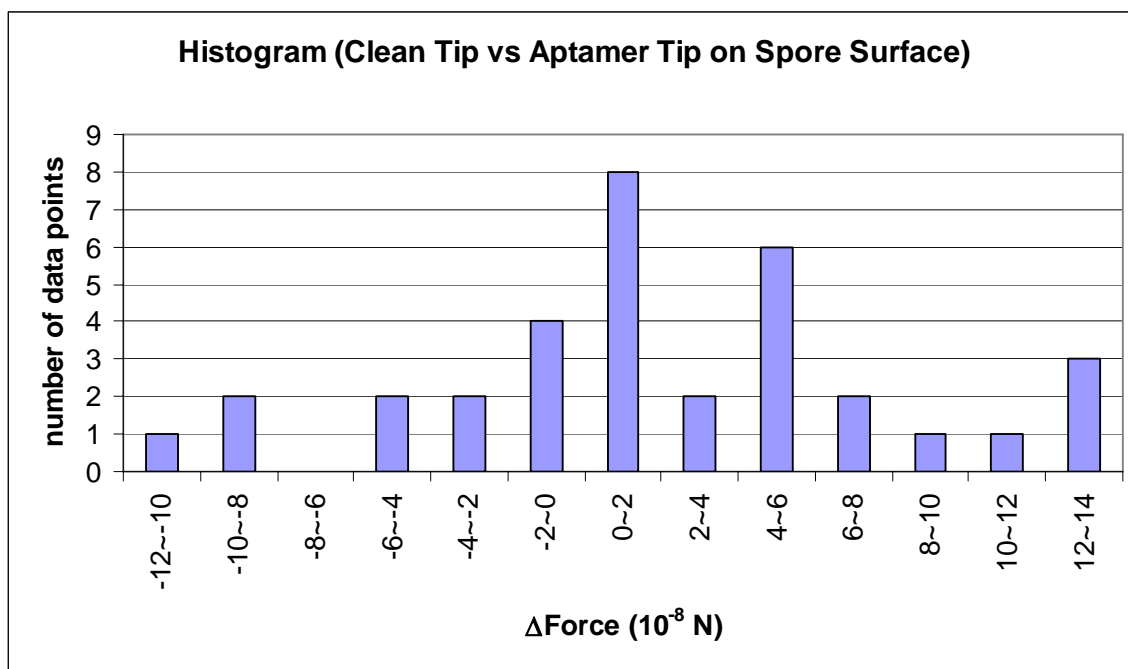
Figure 30. Histogram of difference in forces between clean tips and aptamer tips interacting with a *B. anthracis* spore surface.

Aptamer Tip Interacting with a B. anthracis Spore Surface vs. Clean Tip Interacting with a Blank Surface

Figure 31 represents the difference in force between a clean tip interacting with a *B. anthracis* spore surface and a clean tip interacting with a blank surface. The negative

measurements indicate that the blank surface showed more adhesion than the spore

surface. More can be seen in from a histogram.
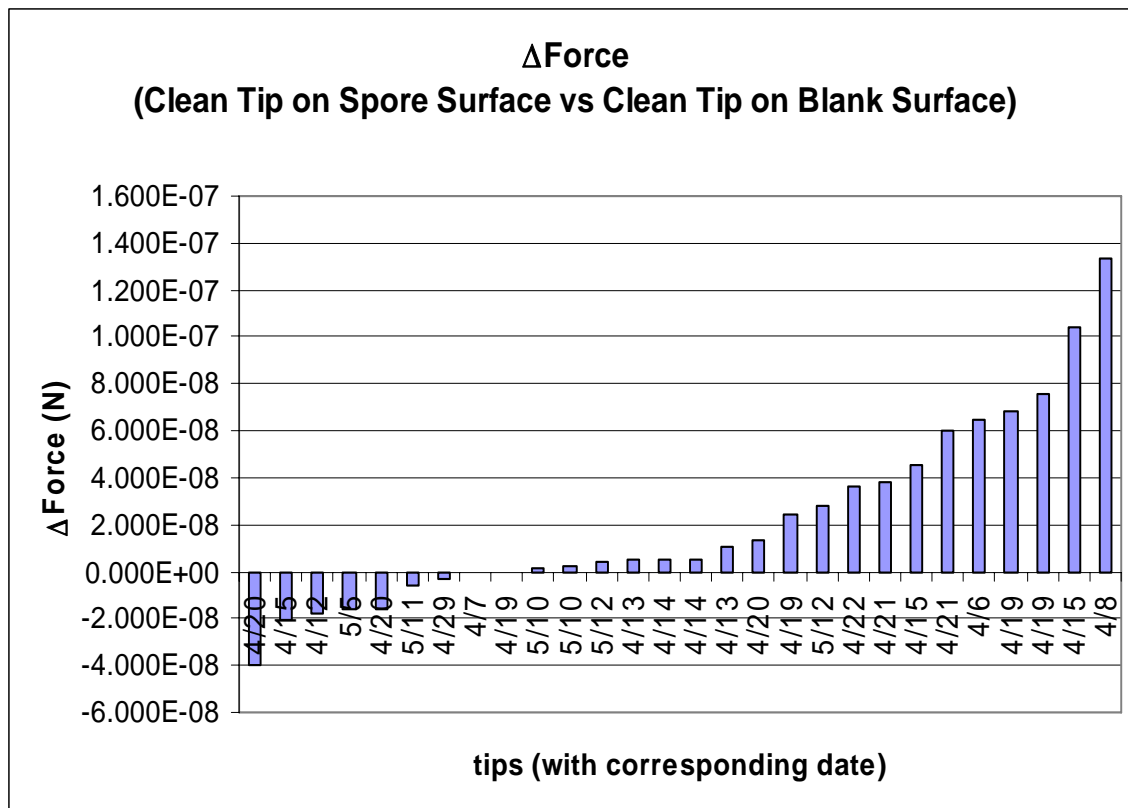
Figure 31. Graph of difference in force between the spore surface and a blank surface
using a clean tip interacting with the *B. anthracis* sample.
The date was added to the x-axis to show that there is no correlation
between the day the data was taken and the adhesion force.

Figure 32 shows a histogram of the data presented from Figure 31. With a clean

tip, the selectivity for the spore surface and the blank surface should be similar. The peak

centered at 0 N shows that there is very little difference in adhesion force between the

spore surface and a blank surface with a clean tip. The peaks at higher forces (4/15 and

4/8) are unaccounted for. This could be from a difference in humidity. The high forces

for these two points correspond with the high forces on the same tip of Figure 29.
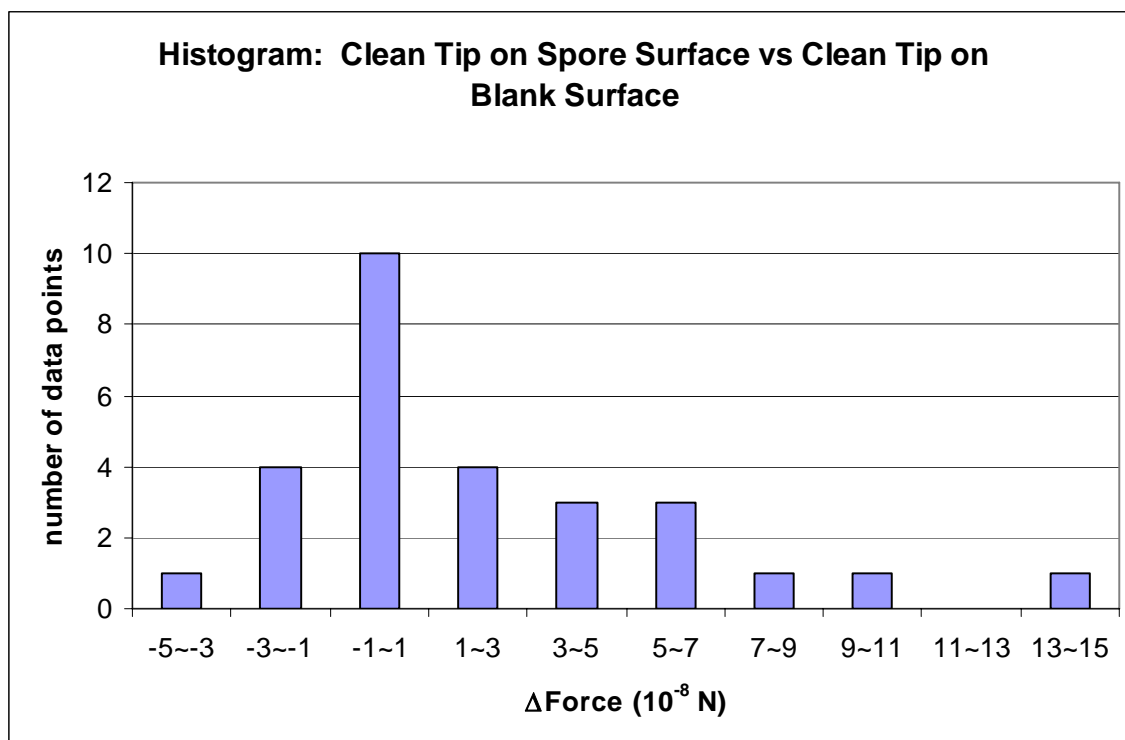
Figure 32. Histogram of difference in forces between the clean tip interacting with a *B. anthracis* spore surface and the clean tip interacting with a blank surface.

Aptamer Tip Interacting with a B. anthracis Spore Surface vs. Clean Tip Interacting with a Blank Surface

Figure 33 represents the difference in force between an aptamer tip interacting with a *B. anthracis* spore surface and a clean tip interacting with a blank surface. The negative measurements indicate that the clean tip interacting with a blank surface showed more adhesion than the aptamer tip interacting with a spore surface. There are similar features in this graph as in the graph of the aptamer tip vs. clean tip interacting with a spore surface. (A comparison can be found in the last section of this chapter.) More can be seen in from a histogram.
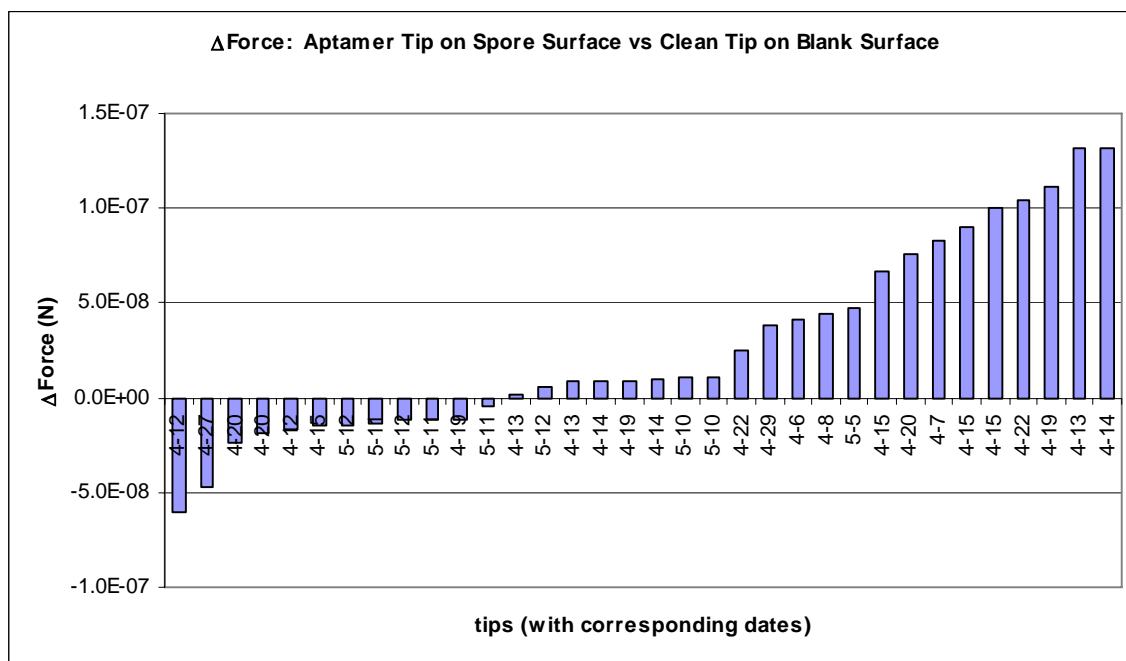
Figure 33. Graph of difference in force between the aptamer tip interacting with a *B. anthracis* spore surface and a clean tip interacting with a blank surface. The date was added to the x-axis to show that there is no correlation between the day the data was taken and the adhesion force.
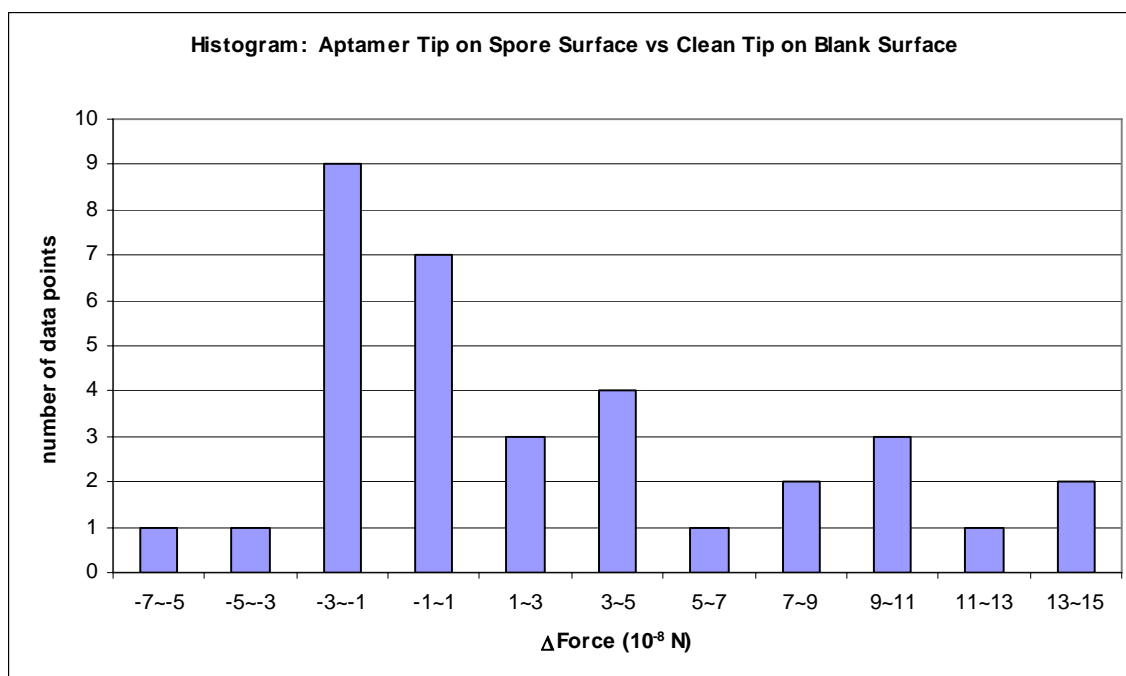
Figure 34. Histogram of difference in forces between the aptamer tip interacting with a *B. anthracis* spore surface and the clean tip interacting with a blank surface.

Figure 34 is a histogram the difference in force between the aptamer tip interacting with a *B. anthracis* spore surface and the clean tip interacting with a blank surface. There are several peaks that show a possibility of the number of aptamers binding to the spore varying.

Results for *B. thuringiensis*

The data in Appendix I is presented in graphical form in the next two sections. It is presented three different ways: clean tip vs. aptamer tip interacting with a *B. thuringiensis* spore surface, clean tip interacting with a *B. thuringiensis* spore surface vs. clean tip interacting with a blank surface, and aptamer tip interacting with a *B. thuringiensis* spore surface vs. clean tip interacting a blank surface.

Clean Tip vs. Aptamer Tip Interacting with a B. thuringiensis Spore Surface

Figure 35 shows a graph of the difference in force between a clean tip and an aptamer tip interacting with a *B. thuringiensis* spore surface. The negative forces indicate that the tip had a larger adhesion force to the spore when it was clean than when aptamers were attached. This demonstrates that the aptamers of *B. anthracis* might not be binding to the spores of *B. thuringiensis*.

Figure 36 shows a histogram of the data presented in Figure 35. Note the distribution centered at 0 N, this implies that there was very little, if any difference in force between the clean tip and the aptamer tip.
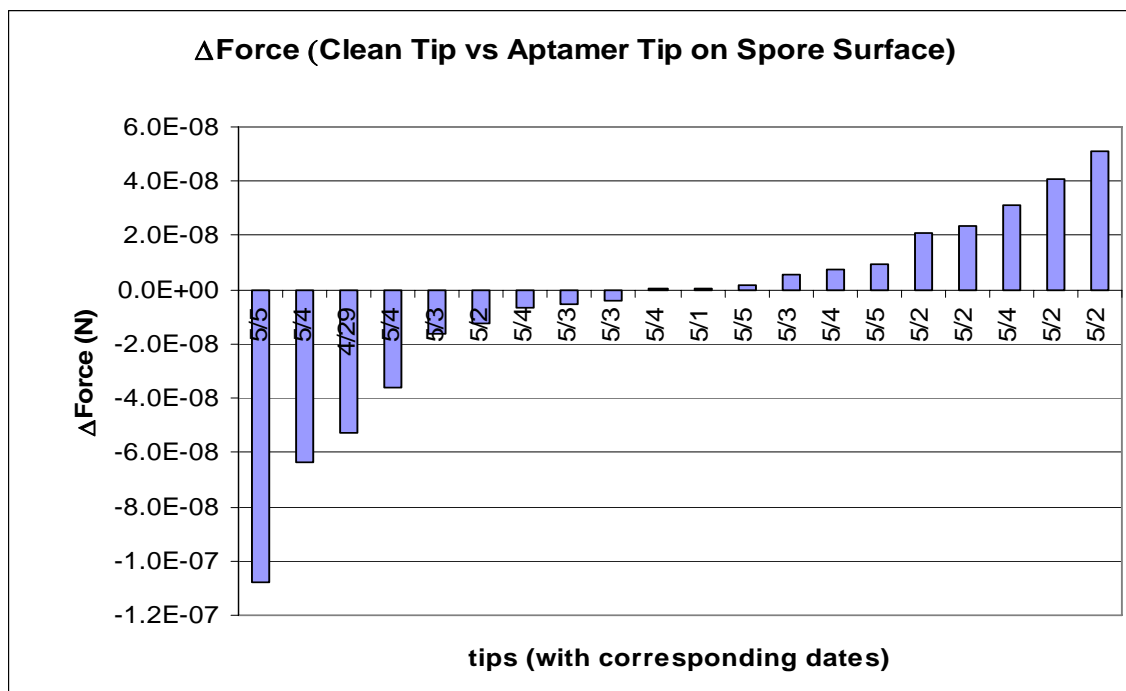
Figure 35. Graph of difference in force between clean tip and aptamer tip for *B. thuringiensis*.
The date was added to the x-axis to show that there is no correlation between the day the data was taken and the adhesion force
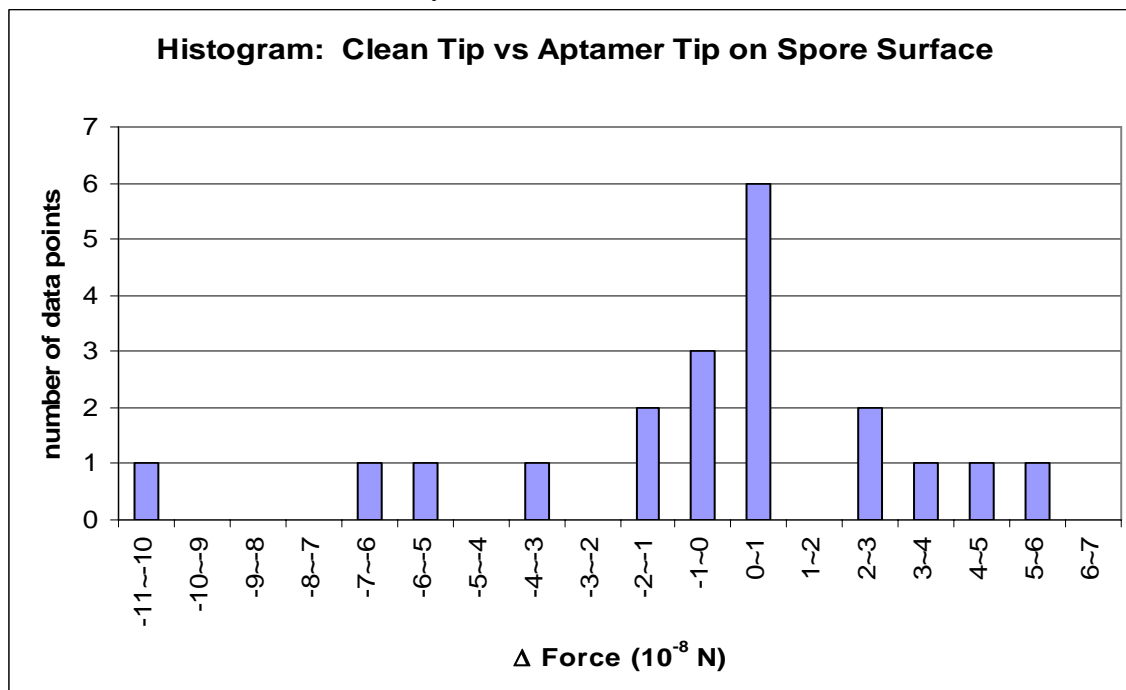
Figure 36. Histogram of difference in forces between clean tips and aptamer tips interacting with a *B. thuringiensis* spore surface.

Aptamer Tip Interacting with a B. thuringiensis Spore Surface vs. Clean Tip Interacting with a Blank Surface

Figure 37 shows the data for the difference in force for a clean tip interacting with the surface of a *B. thuringiensis* spore and a blank surface. The negative forces indicate that the adhesion force to the blank surface was greater than to the spore surface. Figure 38 is a histogram representing the data in Figure 37. Most of the data points appear to near 0 N. This can be seen in the large peak centered at 0 N in. This data shows that there is very little difference in force between the surface of the spore and the blank surface with a clean tip.
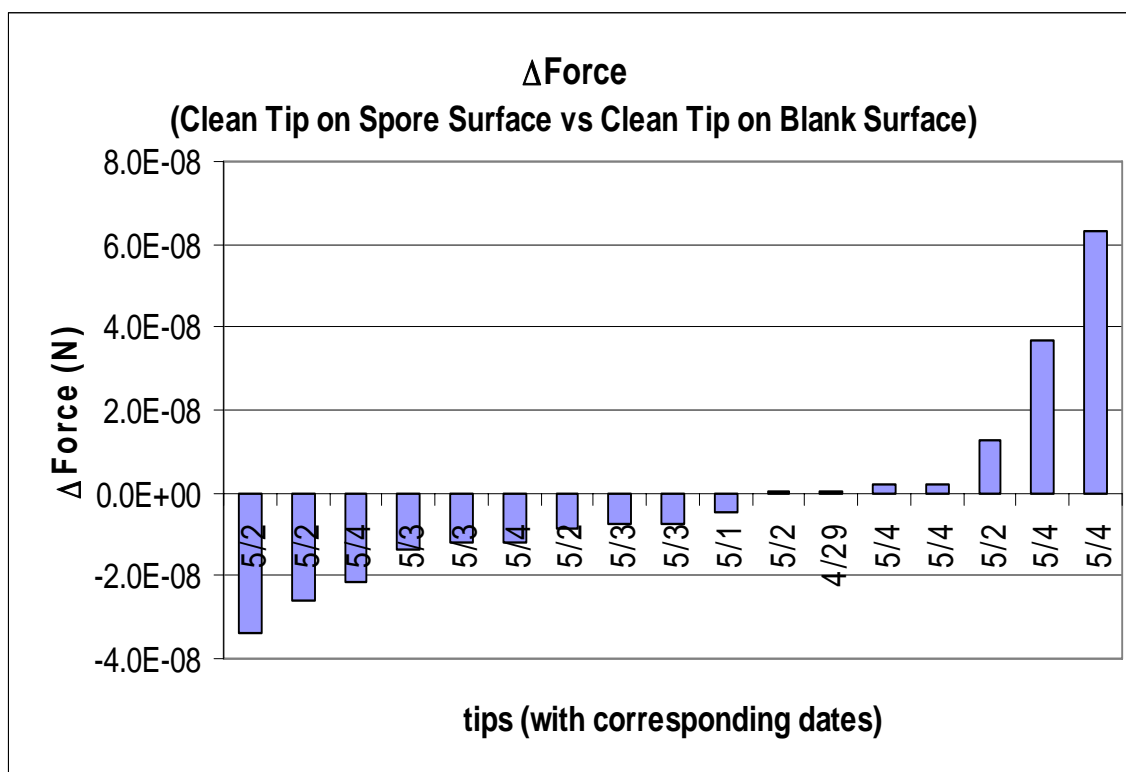
Figure 37. Graph of difference in force between the spore vs. blank with clean tips for *B. thuringiensis*.
The date was added to the x-axis to show that there is no correlation between the day the data was taken and the adhesion force.
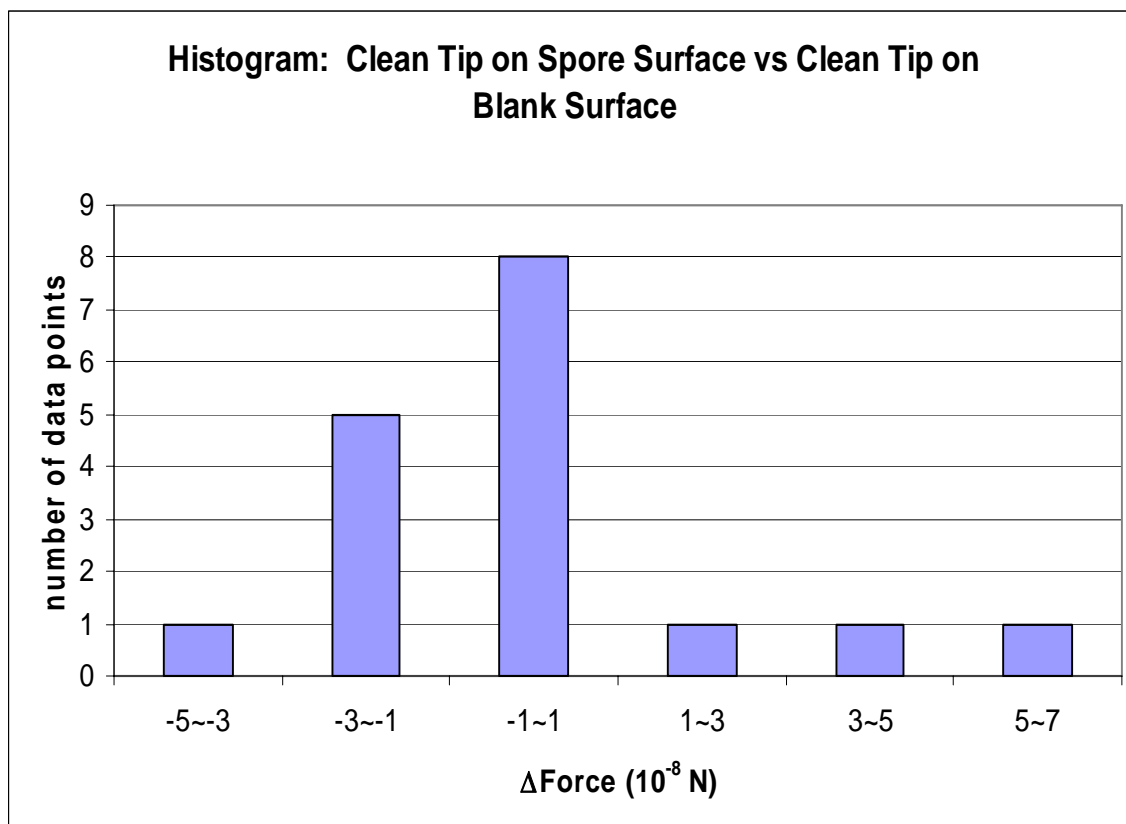
Figure 38. Histogram of difference in forces between a clean tip interacting with a *B. thuringiensis* spore surface and a blank surface.

Aptamer Tip Interacting with a B. thuringiensis Spore Surface vs. Clean Tip Interacting with a Blank Surface

Figure 39 represents the data for the difference in force for aptamer tips interacting with a *B. thuringiensis* spore surface and clean tips interacting with a blank surface. The negative forces indicate that the adhesion force of the clean tip to the blank surface was greater than to the aptamer tip to the spore surface. Figure 40 is a histogram representing the data in Figure 39. Most of the data points appear to near 0 N. This can be seen in the large peak centered at 0 N in. This data shows that there is very little difference in force between the surface of the spore and the blank surface with a clean tip.
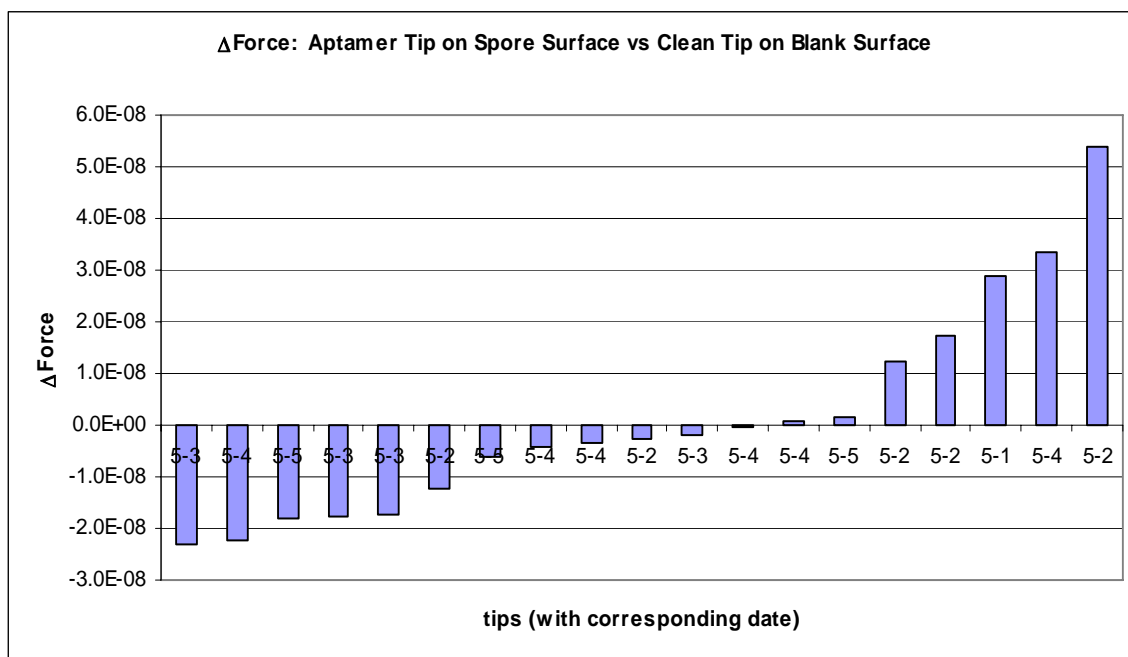
Figure 39. Graph of difference in force between aptamer tip interacting with a *B. thuringiensis* spore surface and clean tip interacting on a blank surface. The date was added to the x-axis to show that there is no correlation between the day the data was taken and the adhesion force
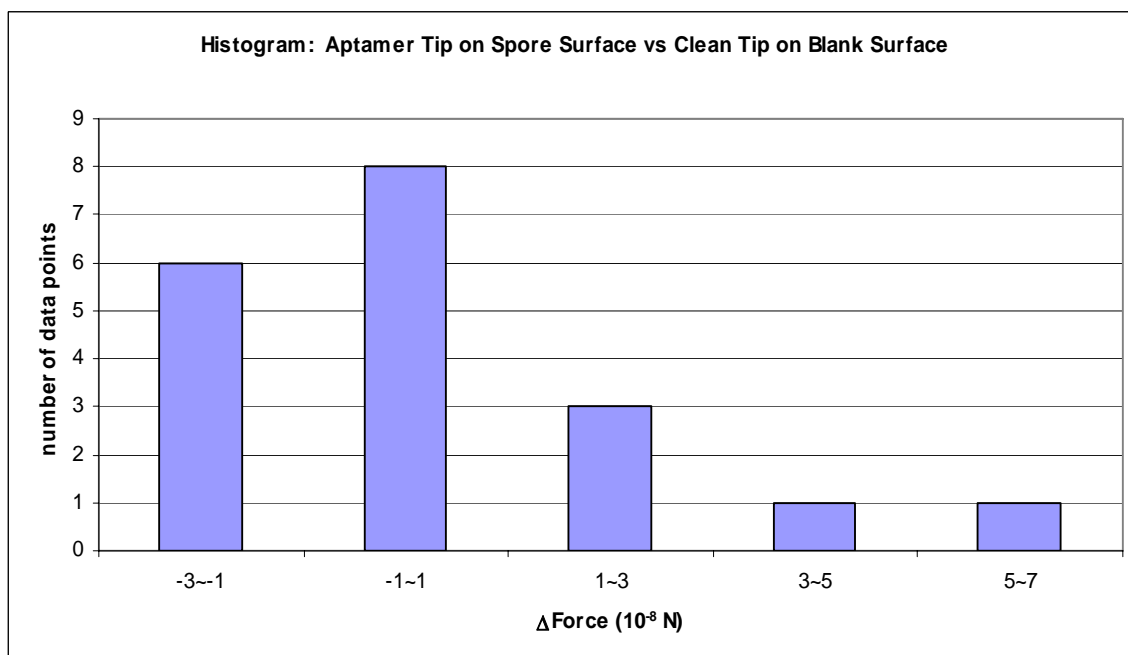
Figure 40. Histogram of difference in forces between aptamer tips interacting with a *B. thuringiensis* spore surface and clean tips interacting with a blank surface.

Side-by-Side Comparison

Figure 41 shows all the difference in force data for *B. anthracis* in one graph. The aptamer tip interacting with a spore surface vs. clean tip interacting with a blank surface (blue diamond) and clean tip and aptamer tip interacting with spore surface (yellow triangle) show similar features, flattening out at similar difference in forces. These similarities indicate that the aptamers are selective for *B. anthracis* spores. The clean tip interacting with both blank surfaces and spores surfaces show similar trend also.

Figure 42 compares the all the data in the form of a histogram. The aptamer tip interacting with a spore surface vs. clean tip interacting with a blank surface (blue) and clean tip vs. aptamer tip interacting with spore surface (yellow) show some similar peak features. The clean tip interacting with the blank surface vs. spore surface shows a peak centered at 0 N.
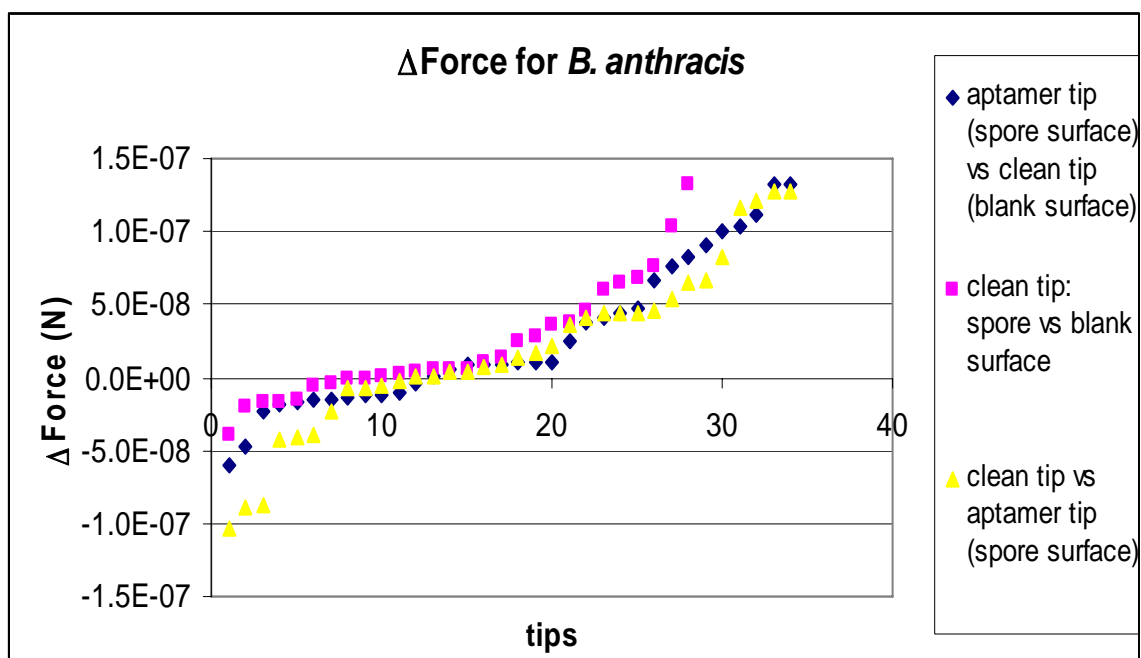
Figure 41. Comparison of difference in forces for *B. anthracis.*
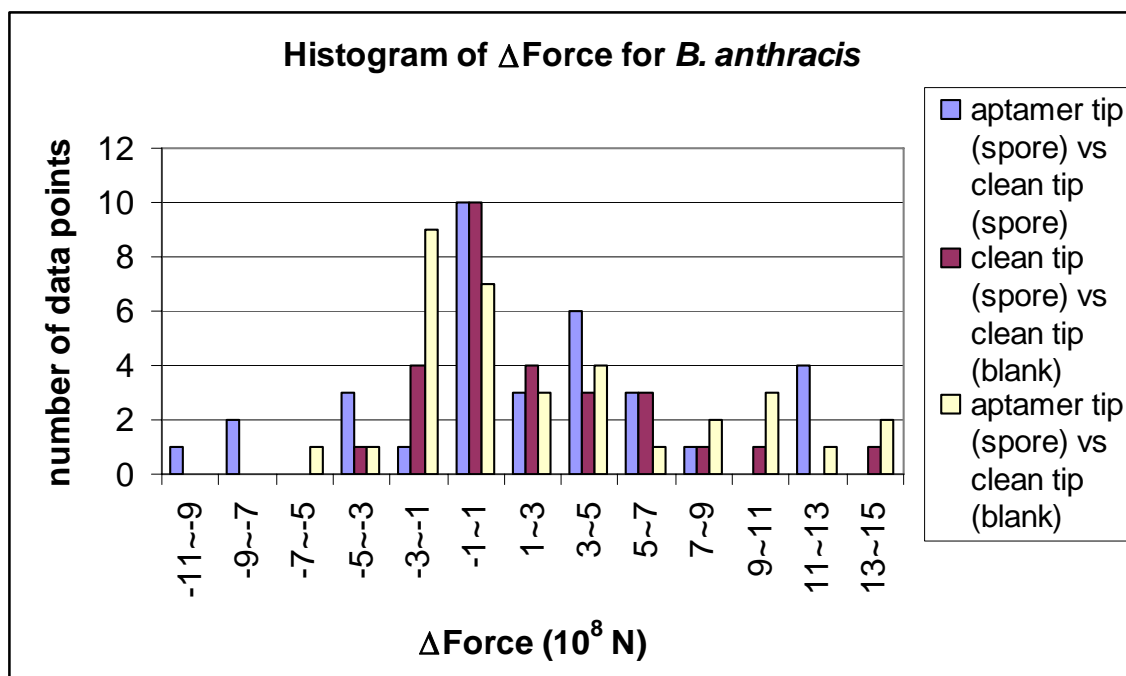
Figure 42. Comparison of histograms for *B. anthracis.*
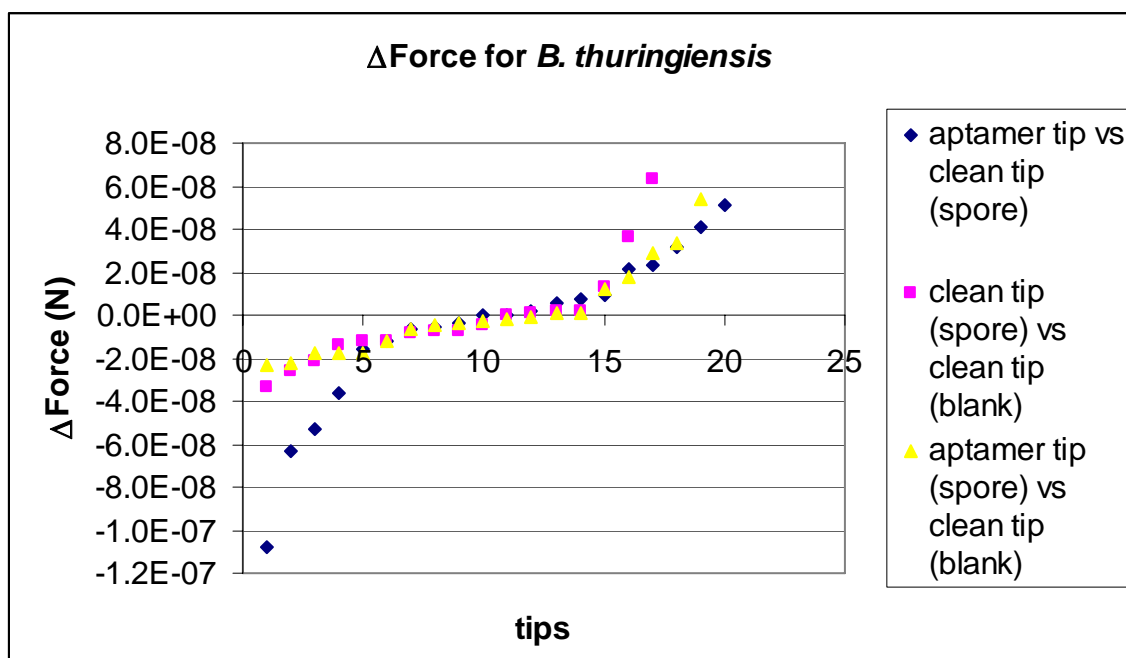
Figure 43. Comparison of difference in forces for *B. thuringiensis.*

Figure 43 shows all the difference in force data for *B. thuringiensis* in one graph.

All three difference in forces have a similar pattern with the aptamer tip vs. clean tip

interacting with the spore surface falling away from this pattern at lower forces. Figure 44 compares all of the data in the form of a histogram. All three difference in forces have a peak centered at 0 N.
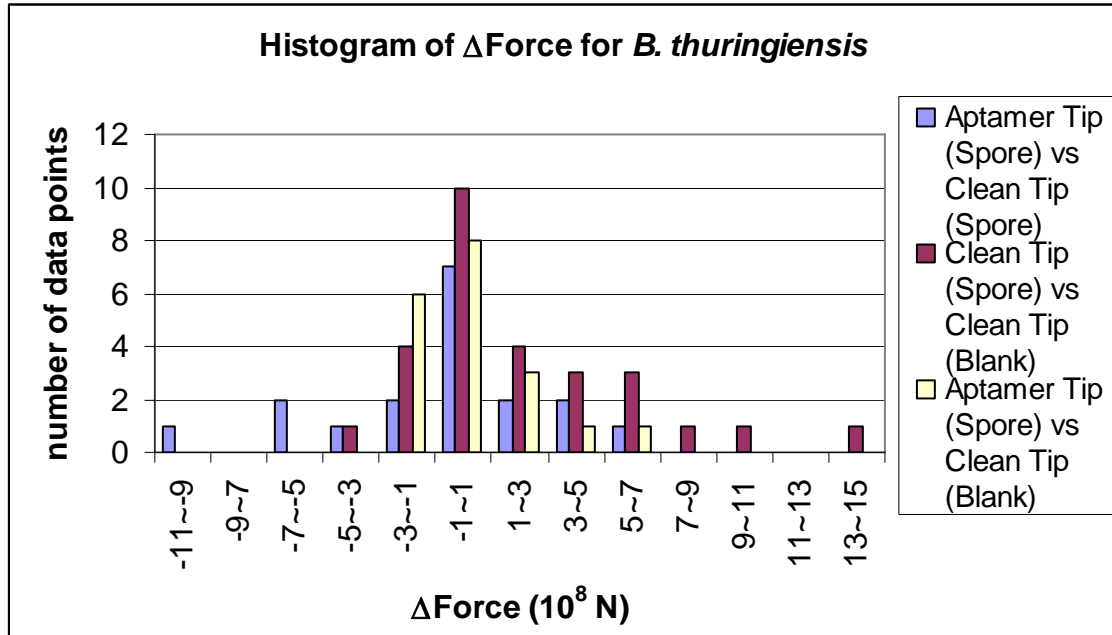
Figure 44. Comparison of histograms for *B. thuringiensis*.

Table 2. Statistics for various difference of forces.

	ΔForce (N)					
	B. anthracis			*B. thuringiensis*		
	aptamer tip vs. clean tip (spore surface)	clean tip spore vs. blank	aptamer tip (spore) vs. clean tip (blank)	aptamer tip vs. clean tip (spore surface)	clean tip spore vs. blank	aptamer tip (spore) vs. clean tip (blank)
Average	1.894E-08	2.160E-08	2.671E-08	-5.604E-09	-1.704E-09	9.482E-10
Standard Deviation	5.775E-08	3.407E-08	5.100E-08	3.706E-08	2.292E-08	2.042E-08
Range	2.305E-07	1.729E-07	1.921E-07	1.591E-07	9.694E-08	7.709E-08
Minimum	-1.037E-07	-3.993E-08	-6.003E-08	-6.361E-08	-3.388E-08	-2.321E-08
Maximum	1.268E-07	1.330E-07	1.321E-07	5.134E-08	6.307E-08	5.388E-08

Table 2 shows the statistics for all the difference in force data. The changes in force for *B. thuringiensis* were all an order of magnitude smaller than that of *B. anthracis*. The aptamer tip vs. clean tip interacting with a spore surface for *B. anthracis* has the

smallest average difference in force, but it also has the largest range and standard

deviation, which accounts for the lower average.

IV. Discussion

Overview

The data collected shows that the aptamers for *B. anthracis* is not selective for spores of *B. thuringiensis*. The data also shows the ability of the aptamer to distinguish of *B. anthracis* from *B. thuringiensis*.

As mentioned earlier, the relative humidity plays a key role in reproducible data. The lack of control of the relativity is one explanation for the large range in all measurements. This appeared to affect the *B. anthracis* data the most since there were larger difference in forces due to aptamer adhesion. This made the range even greater. The larger difference in force measurements for *B. anthracis* all occurred with the same tip. This can be seen with the dates on the x-axis. Low relative humidity may be responsible for this.

For the *B. thuringiensis* data, there was one dominant peak centered at 0 N for the data comparing the clean tip to the aptamer tip. This is to be expected since the aptamer for *B. anthracis* is not selective for *B. thuringiensis*. The data comparing the spore surface to a blank surface also had a dominant peak centered at 0 N. This was as expected since the there is no difference in the selectivity of the spore surface and a blank surface.

The different methods of drying the spore samples didn't appear to affect the data. The *B. thuringiensis* sample which was stored in a desicator acclimated to the new environment fast enough that any differences were not detectable by measurement.

Recommendations for Future Work

In order to get more reproducible measurements, relative humidity measurements should be collected in conjunction with the force. Also, control of the relative humidity could yield an optimal relative humidity for the measurement of the adhesion forces. With higher reproducibility of data, there is a possibility of determining the number of aptamers bound to the spore on each measurement. If available, this experiment can also be repeated with aptamers of *B. thuringiensis* and *B. cereus.*

Other work may include the attaching of aptamers to glass with a silation procedure from Dr. Holwitt of Air Force Research Laboratory in an attempt to build a detector. This will be more useful when the aptamers for other species (*B. thuringiensis* and *B. cereus*) are created.

Conclusions

The use of atomic force microscopy is an effective tool for measuring force. It has allowed for reproducible measurements of adhesion force between aptamers and a spore. As research continues on the contents of the exosporium, a greater understanding of the conformational changes the aptamer undergoes in the binding process with the spore may be achieved. This would give us knowledge of the force required for adhesion of an aptamer to the spore surface.

This research demonstrates that aptamers for *Bacillus* spores may hold the key to quick detection of spores in the event a biological attack. The most efficient means of detection with aptamers is yet to be determined.

Appendix A: SELEX Process

The SELEX process can be broken into eight steps, as seen in Figure 45. 1) A library of single stranded DNA oligonucleotides (a polymer containing 2 - 20 nucleotides) containing a portion of randomized sequence is synthesized. Each oligonucleotide is made up of a 5' and a 3' region of defined sequence and a central region of random sequence. (15: 811) 2) This library is converted into a double strand of DNA by polymerase chain reaction (PCR), a method for making many copies of a specific segment of DNA, using the 5' and 3' constant regions for annealing primers.

  3) The library can be converted into single strand DNA (ssDNA), 3a, or into RNA by in vitro transcription, 3b. 4) Watson-Crick base pairing and noncanonical intramolecular interactions allow each of these ssDNA and RNA sequences to adopt different structures. To isolate the aptamers to a given target molecule, the starting library of nucleic acids is incubated with the molecules of interest. Filtration is used to partition the nucleic acid ligands that bind to the target molecule (5). They are then eluted (6) and amplified by PCR (7). This cycle is repeated until a specific population is achieved.   "On general, around 8-15 cycles of affinity selection and amplification are needed before selecting the "winner" aptamers: an oligonucleotide population that is dominated by those sequences which bind the target best." (15: 811)
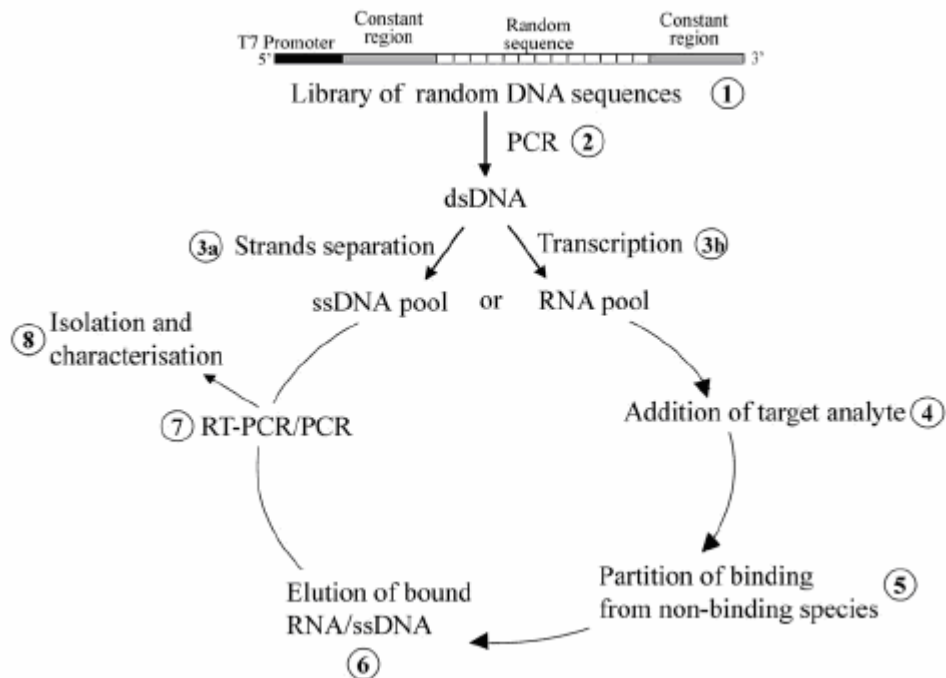
Figure 45. In Vitro Selection of Nucleic Acid Aptamers (SELEX)
(15: 811).

The following figure shows a simplified PCR scheme used in SELEX development

(43:459).
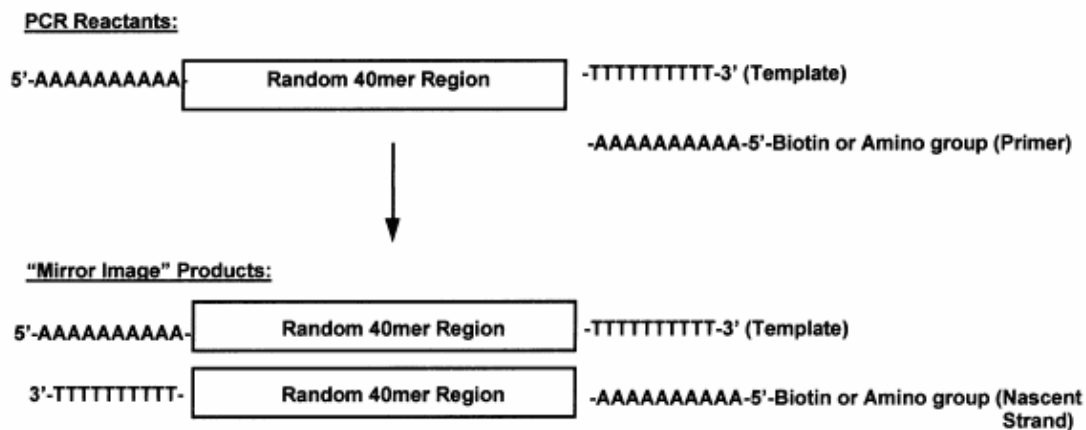
Figure 46. Simplified PCR scheme.
(43: 459).

48

Appendix B: Sporulation

Sporulation of *Bacillus* is a response to nutritional deprivation of carbon and nitrogen sources (30: 85). The bacterial cell makes an inhibitor or repressor from carbon and nitrogen that prevents the initiation of sporulation, so that when either of these two is exhausted, inhibition is released, and the cells sporulate (30: 85).

In stage 0, sporulation is initiated and complete chromosome replication occurs (31: 18). During stage 1 the two nucleoids formed in stage 0 form an axial filament (30: 86). Antibiotics and various enzymes are excreted into the spore (30: 86). Stage 2 is marked by the asymmetrical formation of a double-membrane septum, dividing the cell into a larger mother cell and a smaller forespore (31: 18). "The septum forms before the chromosomes are completely separated, and closes around one of the pair of replicating chromosomes, pinching it into a larger and smaller lobe. The larger chromosome lobe is then transported from the mother cell into the prespore, presumably through a small pore in the septum" (31: 18).
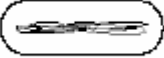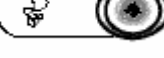
During stage 3, the mother cell develops and engulfs forespore (31: 19). The inner and outer membranes surround the forespore (31: 19). The cell is now committed to sporulation (31: 18). Stage 4 is marked by the forming of the inner cortex between the inner and outerforespore and the forming of the germ cell wall between the cortex and inner forespore membrane (31: 19). Metabolic activity is much less than the vegetative cell (30: 86). The forespore pH is reduced and dehydration begins (31: 19).

In stage 5 spore coat is formed by the deposition of spore coat protein and the forespore continues to dehydrate. (31: 19; 30: 86). During stage 6, the spore core undergoes the

final process of dehydration and the outer spore coat is deposited on the surface of the inner spore coat (31: 20). By the end of this stage, the spore has become metabolically dormant. (31:20). In stage 7, the mother spore releases the mature spore, ending the sporulation process (30: 86).

Table 3. Stages of Sporulation.

Stage 0		Formation of two nucleoids.
Stage 1		Formation of axial filament.
Stage 2		Septum forms.
Stage 3		Mother cell engulfs forespore and spore starts to dehydrate.
Stage 4		Formation of cortex.
Stage 5		Start coat formation
Stage 6		Finish coat formation and dehydration
Stage 7		Maturation

(30: 85).

Appendix C: Contact Mode AFM Force Diagram
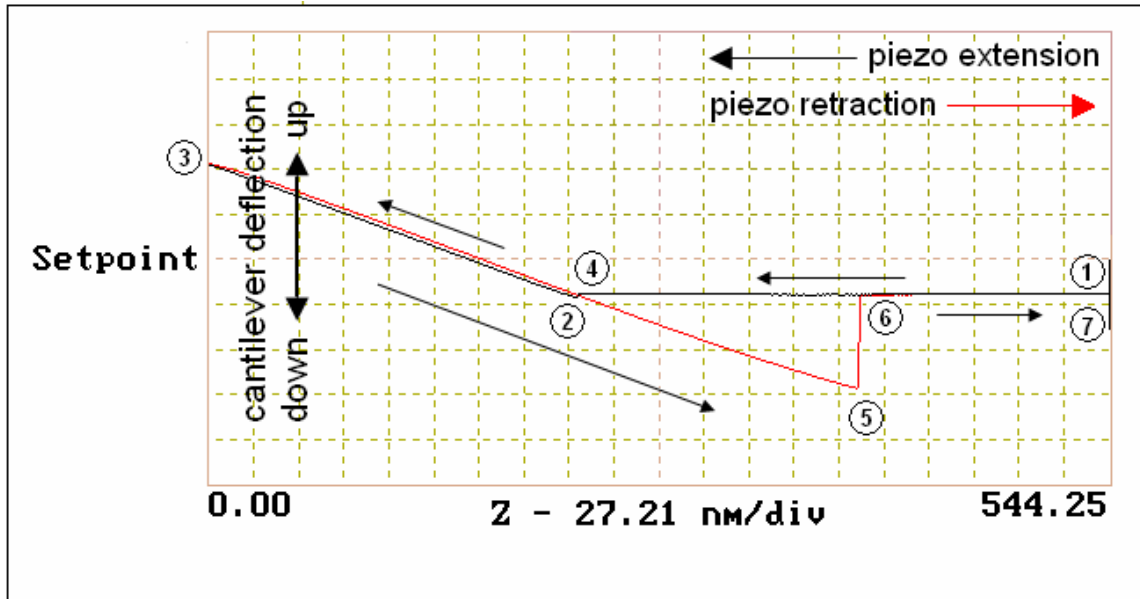
Figure 47. Force diagram showing the tip approaching the surface.

In Figure 47 the piezo extends up and the tip approaches the surface. At point 1, the piezo extends up and the tip descends. There is no contact with the surface yet. At point 2, there is a small dip . The tip is pulled down by attractive forces near the surface. At point 3, the tip presses into the surface and the cantilever bends upward. The piezo retracts and the cantilever relaxes downward, until at point 4, the tip and surface forces are in equilibrium. Between points 4 and 5, the piezo continues to retract and the cantilever bends downward as the surface attraction holds onto the tip. At point 5, the tip is finally released from the surface and the cantilever rebounds upward to point 6. Between points 6 and 7, the piezo continues to retract and the tip ascends. There is no contact with the surface (44: 11.7).

Appendix D: Agar Plate Procedure

Mix 11.5 g Bacto Nutrient Agar with 500 mL dH_2O in a 1 L autoclave bottle. Mix so that all of the Bacto Nutrient Agar is wet. If any part is dry, it will crystallize when autoclaved. Autoclave for 15 minutes at 121ºC and 15 psi. After autoclaving, let the bottle sit at room temperature to cool down. When cooled, put in water bath at 45º for 30 minutes. The plates are ready to be poured. Pour agar into each plate until it is about half full. Be sure not to touch the inside of the plate or the edge of the lid. Replace cover and let sit until agar solidifies. Refrigerate to store.

Appendix E: Gram Stain Procedure

Place one drop of dH$_2$O on a glass slide and mix a small amount of sample (less than one colony) from plate with a loop. Mix well and spread out on slide. Leave slides under hood to dry. This may take up to 30 minutes. The hood was used for faster air flow to aid in the drying process. After the slide dries, heat fix the sample onto the slide. This is done by waving the slide (sample side up) over a flame or incinerator four or five times. The slide should feel warm to touch.

Flood the slide with crystal violet and let sit for one minute. Then rinse with water. Flood the slide with iodine and let sit for one minute. The iodine forms a crystal violet-iodine complex within the cell wall (45). Rinse with water and drop three to five drops of alcohol onto slide to remove excess dye. For Gram positive bacteria, this dehydrates the bacteria, trapping the crystal violet-iodine complex. For Gram negative bacteria, this extracts lipids from the cell wall. This increases the porosity of the cell wall which allows the crystal violet-iodine complex to diffuse from the cell wall (45). Rinse with water and flood with safranin. Let sit for one minute, rinse with water, and let dry. Once dried, the slides are ready for view. Gram-positive bacteria are stained purple. Gram-negative bacteria are stained pink to red (45).

Appendix F: Dilution Series and Spore Count Procedure

Prepare 250 mL of Bacto Nutrient Agar. Mix 5.75 g of Bacto Nutrient Agar and 250 mL dH$_2$O in a 500 mL autoclave bottle. Autoclave for 15 minutes at 121ºC and 15 psi, let cool, and set in 45 ºC water bath for 30 minutes.

Label 10 plates, 2 each with dilution factors of 10^{-3}, 10^{-4}, 10^{-5}, 10^{-6}, and 10^{-7} and set aside. Label eight pop top culture test tubes with dilution factors of 10^{-1} to 10^{-7}. (These work best because they are easy to open with one hand, thus reducing the risk of contamination.) Put 900 µL Bacto Nutrient Broth into each test tube. Add 100 µL sample into test tube labeled 10^{-1}, cap, and vortex for 5 seconds. This dilutes the solution by a tenth. Pipet 100 µL from test tube 10^{-1} to test tube 10^{-2}, cap, and vortex for 5 seconds. Repeat this procedure for all test tubes. Each repetition dilutes the solution by one tenth. For test tube 10^{-7}, remove 100 µL of fluid (so that each tube contains 900 µL of fluid.)

Set aside tubes 10^{-1} and 10^{-2}. Vortex test tube 10^{-3} and pipet 100 µL of test tube 10^{-3} into both plates labeled 10^{-3}. Pour 25 mL Bacto Nutrient Agar into each plate and swirl. Replace lid and let sit for 20 minutes. Repeat last 3 steps for remaining corresponding tubes and plates. After the agar has solidified, incubate at 37ºC for 24 hours, at which time the colonies may be counted.

Appendix G: Dilution Series for Aptamer

Five tubes were labeled 10^{15} through 10^{11}. Add 100 µL dH$_2$O to each tube. In tube 10^{15}, add 10 µL of aptamer sample. Vortex for 5 seconds. Add 10 µL of tube 10^{15} into tube 10^{14} and shake for 5 seconds with Vortex. Repeat this for remaining tubes. Each tube was diluted by a tenth.

Appendix H: Force Calculations for *B. anthracis*

	file	def setpt	mm	Δz	Force (N)	average	variance
clean	406-09	95.49	7.8	1.676E-07	9.720E-08	9.720E-08	
blank	406-11	95.30	2.4	5.146E-08	2.985E-08		
	406-12	94.54	2.8	5.956E-08	3.454E-08	3.220E-08	
dipped	406-13	83.07	6.3	1.178E-07	6.830E-08		
	406-14	85.22	4.5	8.629E-08	5.005E-08		
	406-15	90.77	6.7	1.368E-07	7.936E-08		
	406-16	91.52	6.9	1.421E-07	8.241E-08		
	406-17	97.96	6.9	1.521E-07	8.821E-08	7.366E-08	1.506E-08
blank	406-20	95.07	3.8	8.128E-08	4.715E-08	4.715E-08	
clean	407-03	87.02	3.3	6.461E-08	3.748E-08	3.748E-08	
blank	407-05	91.73	3.2	6.605E-08	3.831E-08	3.831E-08	
dipped	407-06	96.11	3.8	8.217E-08	4.766E-08		
	407-07	96.13	3.3	7.138E-08	4.140E-08		
	407-08	97.59	3.6	7.905E-08	4.585E-08	4.497E-08	3.222E-09
blank	407-11	87.08	2.5	4.898E-08	2.841E-08		
	407-12	89.36	2.5	5.027E-08	2.915E-08	2.878E-08	
clean	407-16	77.95	3.0	5.262E-08	3.052E-08		
	407-17	83.62	2.8	5.268E-08	3.055E-08	3.055E-08	
dipped	407-18	81.05	7.2	1.313E-07	7.615E-08		
	407-19	81.05	7.4	1.349E-07	7.827E-08		
	407-20	80.35	7.1	1.284E-07	7.445E-08		
	407-21	80.35	7.1	1.284E-07	7.445E-08	7.583E-08	1.814E-09
blank	407-23	88.60	3.0	5.981E-08	3.469E-08	3.469E-08	
clean	407-27	78.77	3.7	6.558E-08	3.803E-08		
	407-28	76.27	4.1	7.036E-08	4.081E-08		
	407-29	80.32	4.2	7.590E-08	4.402E-08	4.096E-08	
dipped	407-30	0.13	8.0	2.340E-07	1.357E-07		
	407-31	0.13	8.3	2.428E-07	1.408E-07		
	407-32	80.32	9.0	1.626E-07	9.434E-08	1.236E-07	2.549E-08
blank	407-34	0.11	3.9	9.653E-08	5.598E-08	5.598E-08	
clean	408-03	84.88	14.0	2.674E-07	1.551E-07		
	408-04	85.72	14.0	2.700E-07	1.566E-07		
	408-05	85.72	13.9	2.681E-07	1.555E-07	1.557E-07	7.937E-10
blank	408-07	84.86	2.1	4.010E-08	2.326E-08		
	498-08	89.62	1.9	3.831E-08	2.222E-08	2.274E-08	
dipped	408-09	89.37	2.5	5.027E-08	2.916E-08		
	408-10	92.08	2.6	5.387E-08	3.124E-08		
	408-11	86.12	2.9	5.619E-08	3.259E-08		
	408-12	95.47	10.5	2.255E-07	1.308E-07		
	408-13	89.02	8.7	1.743E-07	1.011E-07		
	408-14	87.08	7.0	1.372E-07	7.955E-08	6.740E-08	4.309E-08
blank	408-16	89.09	3.0	6.014E-08	3.488E-08		
	408-17	83.76	2.7	5.088E-08	2.951E-08	3.220E-08	
clean	408-25	92.52	3.5	7.286E-08	4.226E-08		

	408-26	84.27	2.9	5.499E-08	3.189E-08		
	408-27	93.84	3.0	6.334E-08	3.674E-08		
	408-28	85.73	3.0	5.787E-08	3.356E-08	3.611E-08	4.563E-09
dipped	408-32	99.78	12.0	2.694E-07	1.563E-07		
	408-33	95.80	11.8	2.543E-07	1.475E-07		
	408-34	97.55	11.9	2.612E-07	1.515E-07	1.518E-07	4.373E-09
blank	408-36	0.11	2.0	4.950E-08	2.871E-08		
	408-37	0.10	2.0	4.500E-08	2.610E-08	2.741E-08	
clean	412-08	83.12	15.8	2.955E-07	1.714E-07		
	412-09	80.48	15.7	2.843E-07	1.649E-07		
	412-11	77.51	16.0	2.790E-07	1.618E-07	1.660E-07	4.875E-09
blank	412-12	89.66	5.3	1.069E-07	6.201E-08		
	412-13	85.29	5.5	1.055E-07	6.122E-08		
	412-14	90.61	5.4	1.101E-07	6.385E-08	6.236E-08	1.352E-09
dipped	412-16	98.45	3.5	7.753E-08	4.497E-08		
	412-17	98.16	4.0	8.834E-08	5.124E-08	4.590E-08	
blank	412-19	94.20	3.3	6.994E-08	4.057E-08		
	412-20	93.01	3.3	6.906E-08	4.005E-08		
	412-21	90.95	3.5	7.162E-08	4.154E-08	4.072E-08	7.552E-10
clean	412-25	0.13	5.3	1.550E-07	8.991E-08		
	412-27	0.12	5.9	1.593E-07	9.239E-08	9.115E-08	
blank	412-28	0.12	6.8	1.836E-07	1.065E-07		
	412-29	0.12	7.0	1.890E-07	1.096E-07		
	412-30	0.12	7.0	1.890E-07	1.096E-07	1.086E-07	1.808E-09
dipped	412-35	0.14	2.4	7.560E-08	4.385E-08		
	412-36	0.13	3.0	8.775E-08	5.090E-08		
	412-37	0.13	3.0	8.775E-08	5.090E-08	4.855E-08	4.069E-09
redip	412-42	0.13	2.5	7.313E-08	4.241E-08		
	412-43	0.14	2.8	8.820E-08	5.116E-08		
	412-44	0.13	2.9	8.483E-08	4.920E-08	4.759E-08	4.589E-09
blank	412-45	0.12	3.1	8.370E-08	4.855E-08		
	412-46	0.13	3.0	8.775E-08	5.090E-08		
	412-47	98.16	4.0	8.834E-08	5.124E-08	5.023E-08	1.466E-09
clean	413-11	0.11	4.0	9.900E-08	5.742E-08		
	413-12	0.12	4.0	1.080E-07	6.264E-08	6.003E-08	
blank	413-13	0.13	3.0	8.775E-08	5.090E-08		
	413-14	0.12	3.1	8.370E-08	4.855E-08	4.972E-08	
clean	413-21	89.95	5.7	1.154E-07	6.691E-08		
	413-22	93.87	5.9	1.246E-07	7.228E-08		
	413-23	92.63	5.1	1.063E-07	6.165E-08	6.694E-08	5.313E-09
blank	413-24	89.95	3.0	6.072E-08	3.522E-08		
	413-25	90.04	3.0	6.078E-08	3.525E-08		
	413-26	94.04	3.0	6.348E-08	3.682E-08	3.576E-08	9.145E-10
dipped	413-28	0.10	1.8	4.050E-08	2.349E-08		
	413-29	0.11	2.0	4.950E-08	2.871E-08		
	413-30	0.10	2.1	4.725E-08	2.741E-08	2.654E-08	2.717E-09
clean	414-03	0.11	3.0	7.425E-08	4.307E-08		

	414-04	94.88	2.0	4.270E-08	2.476E-08		
	414-05	94.13	2.0	4.236E-08	2.457E-08		
	414-06	99.78	2.9	6.511E-08	3.776E-08	3.254E-08	9.346E-09
blank	414-07	94.51	2.2	4.678E-08	2.713E-08		
	414-08	98.96	2.0	4.453E-08	2.583E-08		
	414-09	0.10	2.2	4.950E-08	2.871E-08	2.722E-08	1.443E-09
dipped	414-14	80.60	2.8	5.078E-08	2.945E-08		
	414-15	83.12	4.1	7.668E-08	4.447E-08		
	414-16	80.41	3.2	5.790E-08	3.358E-08	3.583E-08	7.761E-09
blank	414-17	94.16	2.6	5.508E-08	3.195E-08		
	414-18	96.09	2.7	5.837E-08	3.386E-08	3.290E-08	
redip	414-21	94.26	2.8	5.938E-08	3.444E-08		
	414-22	93.76	2.1	4.430E-08	2.569E-08		
	414-23	97.02	2.0	4.366E-08	2.532E-08	2.849E-08	5.161E-09
blank	414-24	0.10	4.0	9.000E-08	5.220E-08		
	414-25	0.11	2.9	7.178E-08	4.163E-08	4.691E-08	
redip	414-26	0.10	3.1	6.975E-08	4.046E-08		
	414-27	0.11	2.1	5.198E-08	3.015E-08		
	414-28	0.11	2.8	6.930E-08	4.019E-08	3.693E-08	5.878E-09
blank	414-29	97.78	3.0	6.600E-08	3.828E-08		
	414-30	0.11	3.0	7.425E-08	4.307E-08	4.067E-08	
dipped	414-32	89.64	12.3	2.481E-07	1.439E-07		
	414-33	91.51	13.9	2.862E-07	1.660E-07		
	414-34	90.71	14.2	2.898E-07	1.681E-07	1.593E-07	1.341E-08
blank	414-37	0.11	19.2	4.752E-07	2.756E-07		
	414-38	0.11	9.7	2.401E-07	1.392E-07		
	414-39	0.11	9.9	2.450E-07	1.421E-07	1.857E-07	7.792E-08
clean	414-03	0.11	3.0	7.425E-08	4.307E-08		
	414-04	94.88	2.0	4.270E-08	2.476E-08		
	414-05	94.13	2.0	4.236E-08	2.457E-08		
	414-06	99.78	2.9	6.511E-08	3.776E-08	3.254E-08	9.346E-09
blank	414-07	94.51	2.2	4.678E-08	2.713E-08		
	414-08	98.96	2.0	4.453E-08	2.583E-08		
	414-09	0.10	2.2	4.950E-08	2.871E-08	2.722E-08	1.443E-09
dipped	414-14	80.60	2.8	5.078E-08	2.945E-08		
	414-15	83.12	4.1	7.668E-08	4.447E-08		
	414-16	80.41	3.2	5.790E-08	3.358E-08	3.583E-08	7.761E-09
blank	414-17	94.16	2.6	5.508E-08	3.195E-08		
	414-18	96.09	2.7	5.837E-08	3.386E-08	3.290E-08	
redip	414-21	94.26	2.8	5.938E-08	3.444E-08		
	414-22	93.76	2.1	4.430E-08	2.569E-08		
	414-23	97.02	2.0	4.366E-08	2.532E-08	2.849E-08	5.161E-09
blank	414-24	0.10	4.0	9.000E-08	5.220E-08		
	414-25	0.11	2.9	7.178E-08	4.163E-08	4.691E-08	
redip	414-26	0.10	3.1	6.975E-08	4.046E-08		
	414-27	0.11	2.1	5.198E-08	3.015E-08		
	414-28	0.11	2.8	6.930E-08	4.019E-08	3.693E-08	5.878E-09

blank	414-29	97.78	3.0	6.600E-08	3.828E-08		
	414-30	0.11	3.0	7.425E-08	4.307E-08	4.067E-08	
dipped	414-32	89.64	12.3	2.481E-07	1.439E-07		
	414-33	91.51	13.9	2.862E-07	1.660E-07		
	414-34	90.71	14.2	2.898E-07	1.681E-07	1.593E-07	1.341E-08
blank	414-37	0.11	19.2	4.752E-07	2.756E-07		
	414-38	0.11	9.7	2.401E-07	1.392E-07		
	414-39	0.11	9.9	2.450E-07	1.421E-07	1.857E-07	7.792E-08
clean	415-04	84.41	2.8	5.318E-08	3.084E-08		
	415-05	89.95	2.9	5.869E-08	3.404E-08		
	415-06	91.51	2.7	5.559E-08	3.224E-08	3.238E-08	1.603E-09
blank	415-07	94.22	4.3	9.116E-08	5.287E-08		
	415-08	93.97	4.3	9.092E-08	5.273E-08		
	415-09	94.03	4.3	9.097E-08	5.276E-08	5.279E-08	7.324E-11
dipped	415-10	81.38	11.8	2.161E-07	1.253E-07	1.253E-07	
zoom in	415-12	81.38	13.9	2.545E-07	1.476E-07		
	415-13	82.67	14.2	2.641E-07	1.532E-07		
	415-14	84.33	14.3	2.713E-07	1.574E-07	1.527E-07	4.893E-09
blank	415-18	95.55	3.2	6.880E-08	3.990E-08		
	415-19	88.15	2.8	5.553E-08	3.221E-08	3.606E-08	
clean	415-31	79.50	9.5	1.699E-07	9.856E-08		
	415-32	77.97	9.8	1.719E-07	9.972E-08		
	415-33	77.03	10.1	1.751E-07	1.015E-07	9.994E-08	1.497E-09
blank	415-34	91.38	4.7	9.663E-08	5.605E-08		
	415-35	89.87	4.5	9.099E-08	5.278E-08		
	415-36	91.01	4.5	9.215E-08	5.345E-08	5.409E-08	1.728E-09
dipped	415-37	97.15	8.4	1.836E-07	1.065E-07		
	415-38	94.97	9.7	2.073E-07	1.202E-07		
	415-40	96.95	10.7	2.334E-07	1.354E-07	1.207E-07	1.445E-08
zoom in	415-41	91.04	3.7	7.579E-08	4.396E-08		
	415-42	83.64	4.2	7.904E-08	4.584E-08		
	415-43	86.17	4.0	7.755E-08	4.498E-08		
	415-45	93.60	1.8	3.791E-08	2.199E-08	3.919E-08	1.150E-08
zoom in	415-46	85.82	2.5	4.827E-08	2.800E-08	2.800E-08	
zoom out	415-47	94.61	3.0	6.386E-08	3.704E-08		
	415-48	89.74	2.5	5.048E-08	2.928E-08	3.316E-08	
redip	415-49	0.11	10.1	2.500E-07	1.450E-07		
	415-50	0.11	10.1	2.500E-07	1.450E-07		
	415-51	0.11	10.0	2.475E-07	1.436E-07	1.445E-07	8.288E-10
zoom in	415-52	90.99	2.8	5.732E-08	3.325E-08		
	415-53	95.50	2.0	4.298E-08	2.493E-08	2.909E-08	
blank	415-55	90.06	3.5	7.092E-08	4.113E-08		
	415-56	0.10	3.5	7.875E-08	4.568E-08		
	415-57	95.38	3.1	6.653E-08	3.859E-08	4.180E-08	3.591E-09
clean	419-04	82.48	5.0	9.279E-08	5.382E-08		
	419-05	85.00	5.1	9.754E-08	5.657E-08		

	419-06	84.73	4.6	8.770E-08	5.086E-08	5.375E-08	2.855E-09
dipped	419-07	85.80	2.3	4.440E-08	2.575E-08		
	419-08	85.93	2.8	5.414E-08	3.140E-08		
	419-09	91.71	2.5	5.159E-08	2.992E-08	2.902E-08	2.928E-09
new spore	419-10	77.17	11.3	1.962E-07	1.138E-07		
	419-11	75.00	10.8	1.823E-07	1.057E-07		
	419-12	78.27	10.3	1.814E-07	1.052E-07	1.082E-07	4.823E-09
blank	419-13	96.59	3.0	6.520E-08	3.781E-08		
	419-14	94.62	3.2	6.813E-08	3.951E-08		
	419-15	95.43	3.2	6.871E-08	3.985E-08	3.906E-08	1.091E-09
clean	419-19	91.16	3.1	6.358E-08	3.688E-08		
	419-20	93.11	3.3	6.913E-08	4.010E-08		
	419-21	95.98	3.8	8.206E-08	4.760E-08	4.152E-08	5.499E-09
blank	419-22	95.06	3.3	7.058E-08	4.094E-08		
	419-23	97.72	3.8	8.355E-08	4.846E-08		
	419-24	90.36	3.0	6.099E-08	3.538E-08	4.159E-08	6.566E-09
dipped	419-25	0.12	3.4	9.180E-08	5.324E-08		
	419-26	0.12	3.3	8.910E-08	5.168E-08		
	419-27	0.12	3.0	8.100E-08	4.698E-08	5.063E-08	3.260E-09
blank	419-29	95.66	2.8	6.027E-08	3.495E-08		
	419-30	99.78	2.5	5.613E-08	3.255E-08		
	419-31	92.00	2.8	5.796E-08	3.362E-08	3.371E-08	1.203E-09
clean	419-33	86.68	8.8	1.716E-07	9.954E-08		
	419-34	81.89	11.8	2.174E-07	1.261E-07		
	419-35	81.64	10.1	1.855E-07	1.076E-07	1.111E-07	1.362E-08
blank	419-36	91.63	2.8	5.773E-08	3.348E-08		
	419-37	93.67	3.1	6.533E-08	3.789E-08		
	419-38	90.63	3.0	6.118E-08	3.548E-08	3.562E-08	2.210E-09
dipped	419-39	0.11	2.5	6.188E-08	3.589E-08		
	419-40	0.11	0.3	7.425E-09	4.307E-09		
	419-41	0.11	2.3	5.693E-08	3.302E-08	2.440E-08	1.746E-08
blank	419-43	98.52	2.9	6.428E-08	3.728E-08		
	419-44	99.57	3.0	6.721E-08	3.898E-08		
	419-45	97.51	3.2	7.021E-08	4.072E-08	3.900E-08	1.718E-09
clean	419-46	71.50	10.1	1.625E-07	9.424E-08		
	419-47	71.57	10.3	1.659E-07	9.620E-08		
	419-48	71.59	10.5	1.691E-07	9.810E-08	9.618E-08	1.928E-09
blank	419-50	84.73	2.3	4.385E-08	2.543E-08		
	419-51	85.13	2.8	5.363E-08	3.111E-08	2.827E-08	
dipped	419-52	98.59	10.3	2.285E-07	1.325E-07		
	419-53	0.10	10.0	2.250E-07	1.305E-07		
	419-54	0.10	12.0	2.700E-07	1.566E-07	1.399E-07	1.452E-08
blank	419-56	90.41	2.9	5.899E-08	3.422E-08		
	419-57	90.08	2.5	5.067E-08	2.939E-08		
	419-58	90.90	2.7	5.522E-08	3.203E-08	3.188E-08	2.417E-09
clean	420-01	83.52	4.0	7.517E-08	4.360E-08		

	420-02	82.17	4.0	7.395E-08	4.289E-08		
	420-03	86.64	4.5	8.772E-08	5.088E-08	4.579E-08	4.422E-09
blank	420-04	94.32	7.7	1.634E-07	9.478E-08		
	420-05	89.95	6.7	1.356E-07	7.865E-08		
	420-06	94.37	6.8	1.444E-07	8.374E-08	8.572E-08	8.245E-09
dipped	420-07	97.04	5.0	1.092E-07	6.332E-08		
	420-08	99.01	6.0	1.337E-07	7.752E-08		
	420-09	95.67	4.8	1.033E-07	5.993E-08	6.692E-08	9.336E-09
blank	420-10	86.17	4.7	9.112E-08	5.285E-08		
	420-11	90.10	3.3	6.690E-08	3.880E-08		
	420-12	84.43	3.3	6.269E-08	3.636E-08	4.267E-08	8.901E-09
clean	420-15	77.78	4.0	7.000E-08	4.060E-08		
	420-16	80.45	3.8	6.878E-08	3.990E-08		
	420-17	80.14	4.0	7.213E-08	4.183E-08	4.078E-08	9.808E-10
blank	420-18	91.48	2.2	4.528E-08	2.626E-08		
	420-19	86.87	2.5	4.886E-08	2.834E-08		
	420-20	88.44	2.5	4.975E-08	2.885E-08	2.782E-08	1.371E-09
dipped	420-21	0.11	2.8	6.930E-08	4.019E-08		
	420-22	99.51	1.7	3.806E-08	2.208E-08		
	420-23	0.10	2.1	4.725E-08	2.741E-08	2.989E-08	9.311E-09
new spore	420-25	0.12	8.3	2.241E-07	1.300E-07		
	420-26	0.12	7.8	2.106E-07	1.221E-07		
	420-27	0.10	5.0	1.125E-07	6.525E-08	1.058E-07	3.533E-08
blank	420-28	99.02	3.5	7.798E-08	4.523E-08		
	420-29	95.87	3.0	6.471E-08	3.753E-08	4.138E-08	
clean	420-31	77.62	3.6	6.287E-08	3.647E-08		
	420-32	81.85	2.9	5.341E-08	3.098E-08		
	420-33	80.97	2.8	5.101E-08	2.959E-08	3.234E-08	3.638E-09
blank	420-34	89.99	4.8	9.719E-08	5.637E-08		
	420-35	89.72	5.0	1.009E-07	5.854E-08		
	420-36	88.38	2.6	5.170E-08	2.999E-08	4.830E-08	1.590E-08
dipped	420-40	0.11	1.8	4.455E-08	2.584E-08		
	420-41	0.11	1.8	4.455E-08	2.584E-08		
	420-42	0.10	1.7	3.825E-08	2.219E-08	2.462E-08	2.110E-09
blank	420-43	99.02	2.6	5.793E-08	3.360E-08	3.360E-08	
clean	421-01	73.15	8.0	1.317E-07	7.637E-08		
	421-02	74.41	8.9	1.490E-07	8.642E-08		
	421-03	73.45	9.0	1.487E-07	8.627E-08	8.302E-08	5.761E-09
blank	421-04	87.23	3.5	6.869E-08	3.984E-08		
	421-05	92.23	4.0	8.301E-08	4.814E-08		
	421-06	91.88	3.9	8.062E-08	4.676E-08	4.492E-08	4.448E-09
dipped	421-09	82.60	3.3	6.133E-08	3.557E-08		
	421-10	82.82	3.2	5.963E-08	3.459E-08		
	421-11	84.66	3.2	6.096E-08	3.535E-08	3.517E-08	5.180E-10
redipped	421-12	79.99	4.6	8.279E-08	4.802E-08		
	421-13	80.21	5.5	9.926E-08	5.757E-08		

	421-14	78.11	5.8	1.019E-07	5.912E-08	5.490E-08	6.013E-09
new spore	421-16	82.23	6.2	1.147E-07	6.653E-08		
	421-17	82.23	7.5	1.388E-07	8.048E-08		
	421-18	85.56	8.1	1.559E-07	9.044E-08		
	421-19	85.96	7.8	1.509E-07	8.750E-08	8.124E-08	1.066E-08
blank	421-20	84.84	3.8	7.254E-08	4.207E-08		
	421-21	88.56	4.0	7.970E-08	4.623E-08		
	421-22	88.38	3.9	7.755E-08	4.498E-08	4.443E-08	2.133E-09
clean	421-25	76.16	9.3	1.594E-07	9.243E-08		
	421-26	77.84	8.3	1.454E-07	8.431E-08		
	421-27	77.55	7.2	1.256E-07	7.287E-08	8.320E-08	9.830E-09
blank	421-28	87.74	1.7	3.356E-08	1.947E-08		
	421-29	89.82	2.0	4.042E-08	2.344E-08		
	421-30	88.81	2.2	4.396E-08	2.550E-08	2.280E-08	3.067E-09
dipped	421-31	0.10	2.5	5.625E-08	3.263E-08		
	421-32	0.10	3.2	7.200E-08	4.176E-08		
	421-33	0.10	2.6	5.850E-08	3.393E-08	3.611E-08	4.941E-09
new spore	421-34	0.12	2.2	5.940E-08	3.445E-08		
	421-35	0.11	2.8	6.930E-08	4.019E-08		
	421-36	0.12	3.2	8.640E-08	5.011E-08	4.159E-08	7.922E-09
blank	421-38	92.47	7.8	1.623E-07	9.413E-08		
	421-39	91.59	7.8	1.607E-07	9.323E-08		
	421-40	90.78	7.4	1.514E-07	8.778E-08	9.171E-08	3.431E-09
clean	422-00	91.50	4.1	8.441E-08	4.896E-08		
	422-01	91.48	4.5	9.262E-08	5.372E-08		
	422-02	88.77	4.5	8.988E-08	5.213E-08	5.160E-08	2.426E-09
blank	422-04	38.57	4.5	3.905E-08	2.265E-08		
	422-05	39.39	2.8	2.482E-08	1.439E-08		
	422-06	41.02	1.8	1.661E-08	9.636E-09	1.556E-08	6.585E-09
clean	422-07	79.47	4.9	8.762E-08	5.082E-08		
	422-08	79.33	5.0	8.925E-08	5.176E-08		
	422-09	77.10	5.5	9.541E-08	5.534E-08	5.264E-08	2.385E-09
dipped	422-11	90.25	3.5	7.107E-08	4.122E-08		
	422-12	90.34	3.2	6.504E-08	3.773E-08		
	422-13	90.36	3.5	7.116E-08	4.127E-08	4.007E-08	2.033E-09
new spore	422-15	0.11	7.8	1.931E-07	1.120E-07		
	422-16	0.12	8.1	2.187E-07	1.268E-07	1.194E-07	
blank	422-18	86.30	4.1	7.961E-08	4.617E-08		
	422-19	89.73	4.2	8.479E-08	4.918E-08		
	422-20	90.32	4.3	8.738E-08	5.068E-08	4.868E-08	2.296E-09
clean	427-01	82.91	3.2	5.970E-08	3.462E-08		
	427-02	82.95	3.2	5.972E-08	3.464E-08		
	427-03	83.71	3.6	6.781E-08	3.933E-08		
	427-04	86.85	3.8	7.426E-08	4.307E-08		
	427-05	86.51	3.9	7.591E-08	4.403E-08		

	427-06	83.60	3.8	7.148E-08	4.146E-08	3.952E-08	4.111E-09
blank	427-07	87.34	6.8	1.336E-07	7.751E-08		
	427-08	91.53	6.8	1.400E-07	8.122E-08		
	427-09	91.46	7.0	1.440E-07	8.355E-08		
	427-10	92.52	6.9	1.436E-07	8.331E-08		
	427-11	92.08	6.7	1.388E-07	8.051E-08		
	427-12	90.36	6.7	1.362E-07	7.901E-08	8.085E-08	2.374E-09
dipped	427-13	0.15	1.3	4.388E-08	2.545E-08		
	427-14	0.15	1.1	3.713E-08	2.153E-08		
	427-15	0.15	1.0	3.375E-08	1.958E-08		
	427-16	0.16	1.0	3.600E-08	2.088E-08		
	427-17	0.16	0.9	3.240E-08	1.879E-08		
	427-18	0.16	0.9	3.240E-08	1.879E-08	2.084E-08	2.518E-09
new spore	427-20	0.13	3.3	9.653E-08	5.598E-08		
	427-21	0.14	2.3	7.245E-08	4.202E-08		
	427-22	0.14	1.4	4.410E-08	2.558E-08		
	427-23	0.14	1.7	5.355E-08	3.106E-08		
	427-24	0.13	1.4	4.095E-08	2.375E-08		
	427-25	0.13	1.3	3.803E-08	2.205E-08	3.341E-08	1.321E-08
blank	427-26	0.16	1.1	3.960E-08	2.297E-08		
	427-27	0.15	1.0	3.375E-08	1.958E-08		
	427-28	0.15	1.0	3.375E-08	1.958E-08		
	427-29	0.15	1.2	4.050E-08	2.349E-08		
	427-30	0.14	1.1	3.465E-08	2.010E-08		
	427-31	0.15	1.1	3.713E-08	2.153E-08	2.121E-08	1.731E-09
clean	429-01	79.50	4.1	7.334E-08	4.254E-08		
	429-02	86.79	3.0	5.858E-08	3.398E-08		
	429-03	87.74	2.8	5.528E-08	3.206E-08	3.619E-08	5.578E-09
blank	429-04	97.07	3.5	7.644E-08	4.434E-08		
	429-05	95.69	3.0	6.459E-08	3.746E-08		
	429-06	94.03	3.0	6.347E-08	3.681E-08	3.954E-08	4.169E-09
dipped	429-07	89.13	3.0	6.016E-08	3.489E-08		
	429-08	91.95	4.9	1.014E-07	5.880E-08		
	429-09	93.76	5.7	1.202E-07	6.974E-08		
	429-10	93.60	7.0	1.474E-07	8.550E-08		
	429-11	93.08	8.9	1.864E-07	1.081E-07		
	429-12	96.42	8.5	1.844E-07	1.070E-07	7.733E-08	2.861E-08
blank	420-15	95.12	2.2	4.708E-08	2.731E-08		
	420-16	92.52	2.1	4.372E-08	2.536E-08		
	420-17	92.89	2.0	4.180E-08	2.424E-08	2.564E-08	1.552E-09
clean	505-01	96.58	2.4	5.215E-08	3.025E-08		
	505-02	93.76	2.3	4.852E-08	2.814E-08	2.920E-08	1.490E-09
blank	505-04	97.04	4.8	1.048E-07	6.079E-08		
	505-05	94.50	3.0	6.379E-08	3.700E-08		
	505-06	91.72	3.2	6.604E-08	3.830E-08	4.536E-08	1.337E-08
dipped	505-07	0.12	4.3	1.161E-07	6.734E-08		

	505-08	0.14	8.1	2.552E-07	1.480E-07		
	505-09	0.13	1.8	5.265E-08	3.054E-08		
	505-10	0.11	7.7	1.906E-07	1.105E-07		
	505-11	0.11	7.5	1.856E-07	1.077E-07	9.281E-08	4.502E-08
blank	505-13	0.11	3.2	7.920E-08	4.594E-08		
	505-14	0.11	3.2	7.920E-08	4.594E-08		
	505-15	0.11	3.0	7.425E-08	4.307E-08	4.498E-08	1.658E-09

64

Appendix I: Force Calculations for *B. thuringiensis*

	file	def setpt	mm	Δz	Force (N)	average	variance
clean	429-01	42.94	4.3	4.154E-08	2.410E-08		
	429-02	42.64	4.4	4.221E-08	2.448E-08		
	429-03	43.75	6.5	6.398E-08	3.711E-08	2.856E-08	7.405E-09
blank	429-04	42.99	4.8	4.643E-08	2.693E-08		
	429-05	43.81	5.1	5.027E-08	2.916E-08	2.804E-08	
dipped	429-07	50.63	12.1	1.378E-07	7.995E-08		
	429-08	51.73	11.0	1.280E-07	7.426E-08		
	429-09	49.76	12.6	1.411E-07	8.182E-08	7.868E-08	3.938E-09
blank	429-10	48.74	3.8	4.167E-08	2.417E-08		
	429-11	48.70	3.9	4.273E-08	2.479E-08		
	429-12	48.41	4.4	4.841E-08	2.808E-08	2.568E-08	2.101E-09
clean	501-00	44.92	2.7	2.729E-08	1.583E-08		
	501-01	46.39	2.5	2.609E-08	1.513E-08		
	501-02	45.65	3.0	3.081E-08	1.787E-08	1.628E-08	1.423E-09
blank	501-05	47.87	3.8	4.093E-08	2.374E-08		
	501-06	48.50	3.3	3.601E-08	2.089E-08		
	501-07	47.13	3.0	3.181E-08	1.845E-08	2.103E-08	2.646E-09
dipped	501-08	41.05	9.0	8.313E-08	4.821E-08		
	501-09	41.68	9.5	8.909E-08	5.167E-08		
	501-10	41.20	9.3	8.621E-08	5.000E-08	4.996E-08	1.730E-09
blank	501-12	45.44	3.6	3.681E-08	2.135E-08		
	501-13	45.22	3.9	3.968E-08	2.301E-08		
	501-14	46.88	4.0	4.219E-08	2.447E-08	2.294E-08	1.563E-09
clean	502-01	85.97	2.5	4.836E-08	2.805E-08		
	502-02	85.28	4.0	7.675E-08	4.452E-08		
	502-03	87.49	3.9	7.677E-08	4.453E-08	3.903E-08	9.511E-09
blank	502-04	85.97	3.8	7.350E-08	4.263E-08		
	502-05	87.62	3.4	6.703E-08	3.888E-08		
	502-06	88.83	3.0	5.996E-08	3.478E-08	3.876E-08	3.929E-09
dipped	502-07	0.10	2.3	5.175E-08	3.002E-08		
	502-08	0.10	2.0	4.500E-08	2.610E-08		
	502-09	99.53	1.8	4.031E-08	2.338E-08	2.650E-08	3.336E-09
blank	502-10	97.49	4.4	9.652E-08	5.598E-08		
	502-11	97.39	4.8	1.052E-07	6.101E-08		
	502-12	96.81	5.0	1.089E-07	6.317E-08	6.005E-08	3.689E-09
clean	502-15	88.89	3.0	6.000E-08	3.480E-08		
	502-16	87.29	3.0	5.892E-08	3.417E-08		
	502-17	92.22	2.9	6.017E-08	3.490E-08	3.463E-08	3.938E-10
blank	502-18	87.02	2.8	5.482E-08	3.180E-08		
	502-19	86.95	1.5	2.935E-08	1.702E-08		
	502-20	83.76	1.5	2.827E-08	1.640E-08	2.174E-08	8.717E-09
dipped	502-21	89.28	6.0	1.205E-07	6.991E-08		
	502-22	91.41	6.2	1.275E-07	7.396E-08		

	502-23	89.55	7.1	1.431E-07	8.297E-08	7.561E-08	6.688E-09
clean	502-25	88.61	2.8	5.582E-08	3.238E-08		
	502-26	88.21	2.2	4.366E-08	2.533E-08		
	502-27	88.59	2.9	5.780E-08	3.353E-08	3.041E-08	4.441E-09
blank	502-28	86.35	4.9	9.520E-08	5.522E-08		
	502-29	87.66	4.9	9.665E-08	5.605E-08		
	502-30	89.95	5.0	1.012E-07	5.869E-08	5.665E-08	1.814E-09
dipped	502-31	92.75	4.2	8.765E-08	5.084E-08		
	502-32	92.61	4.5	9.377E-08	5.439E-08		
	502-33	93.69	4.6	9.697E-08	5.624E-08	5.382E-08	2.747E-09
blank	502-35	97.41	3.0	6.575E-08	3.814E-08		
	502-36	91.81	3.6	7.437E-08	4.313E-08		
	502-37	93.73	3.7	7.803E-08	4.526E-08	4.218E-08	3.656E-09
clean	502-39	93.88	3.2	6.759E-08	3.920E-08		
	502-40	93.30	3.0	6.298E-08	3.653E-08		
	502-41	91.69	3.1	6.395E-08	3.709E-08	3.761E-08	1.411E-09
blank	502-42	94.17	3.2	6.780E-08	3.933E-08		
	502-43	96.58	3.2	6.954E-08	4.033E-08		
	502-44	96.12	4.7	1.016E-07	5.896E-08	4.620E-08	1.105E-08
dipped	502-45	92.08	4.7	9.737E-08	5.648E-08		
	502-46	95.10	4.9	1.048E-07	6.081E-08	5.864E-08	3.065E-09
blank	502-49	99.33	2.3	5.140E-08	2.981E-08		
	502-51	99.61	2.4	5.379E-08	3.120E-08	3.051E-08	9.786E-10
clean	502-53	77.54	1.8	3.140E-08	1.821E-08		
	502-54	87.33	1.6	3.144E-08	1.823E-08		
	502-55	75.82	5.0	8.530E-08	4.947E-08	2.864E-08	1.804E-08
blank	502-56	88.65	5.8	1.157E-07	6.710E-08		
	502-57	89.08	5.0	1.002E-07	5.812E-08		
	502-58	88.44	5.4	1.075E-07	6.232E-08	6.252E-08	4.490E-09
dipped	502-59	98.16	6.2	1.369E-07	7.942E-08		
	502-60	0.10	6.1	1.373E-07	7.961E-08		
	502-61	0.10	6.2	1.395E-07	8.091E-08	7.998E-08	8.117E-10
blank	502-63	0.13	2.3	6.728E-08	3.902E-08		
	502-64	0.12	2.7	7.290E-08	4.228E-08		
	502-65	0.13	2.1	6.143E-08	3.563E-08	3.898E-08	3.328E-09
clean	503-01	84.34	2.8	5.313E-08	3.082E-08		
	503-02	87.97	2.5	4.948E-08	2.870E-08	2.976E-08	1.497E-09
blank	503-04	88.17	4.0	7.935E-08	4.602E-08		
	503-05	89.96	3.8	7.692E-08	4.461E-08		
	503-06	86.52	3.1	6.035E-08	3.500E-08	4.188E-08	5.998E-09
dipped	503-07	87.69	2.0	3.946E-08	2.289E-08		
	503-08	90.85	2.0	4.088E-08	2.371E-08		
	503-09	90.71	2.2	4.490E-08	2.604E-08	2.421E-08	1.637E-09
blank	503-11	87.62	3.0	5.914E-08	3.430E-08		
	503-12	85.25	3.2	6.138E-08	3.560E-08		
	503-13	88.91	3.8	7.602E-08	4.409E-08	3.800E-08	5.316E-09
clean	503-15	87.83	3.5	6.917E-08	4.012E-08		

	503-16	84.48	3.1	5.892E-08	3.418E-08		
	503-17	86.37	3.2	6.219E-08	3.607E-08	3.679E-08	3.035E-09
blank	503-18	87.96	4.4	8.708E-08	5.051E-08		
	503-19	87.77	4.0	7.899E-08	4.582E-08		
	503-20	89.04	4.7	9.416E-08	5.461E-08	5.031E-08	4.402E-09
dipped	503-21	0.11	2.6	6.435E-08	3.732E-08		
	503-22	0.12		0.000E+00	0.000E+00		
	503-23	0.11	2.0	4.950E-08	2.871E-08	3.302E-08	1.954E-08
blank	503-25	0.11	3.2	7.920E-08	4.594E-08		
	503-26	0.11	3.5	8.663E-08	5.024E-08		
	503-27	0.11	3.5	8.663E-08	5.024E-08	4.881E-08	2.486E-09
clean	503-29	86.40	4.0	7.776E-08	4.510E-08		
	503-30	89.66	3.1	6.254E-08	3.627E-08		
	503-31	89.17	3.6	7.223E-08	4.189E-08	4.109E-08	4.469E-09
blank	503-32	85.60	4.0	7.704E-08	4.468E-08		
	503-33	87.47	4.4	8.660E-08	5.023E-08		
	503-34	85.15	4.5	8.621E-08	5.000E-08	4.830E-08	3.138E-09
dipped	503-35	97.14	1.9	4.153E-08	2.409E-08		
	503-36	96.11	2.0	4.325E-08	2.508E-08		
	503-37	0.10	2.0	4.500E-08	2.610E-08	2.509E-08	1.007E-09
blank	503-39	0.11	2.0	4.950E-08	2.871E-08		
	503-40	0.11	1.9	4.703E-08	2.727E-08		
	503-41	0.10	1.9	4.275E-08	2.480E-08	2.693E-08	1.981E-09
clean	503-43	83.56	1.8	3.384E-08	1.963E-08		
	503-44	80.92	2.0	3.641E-08	2.112E-08		
	503-45	84.05	2.0	3.782E-08	2.194E-08	2.090E-08	1.171E-09
blank	503-46	87.01	2.0	3.915E-08	2.271E-08		
	503-47	87.62	2.5	4.929E-08	2.859E-08		
	503-48	87.76	2.9	5.726E-08	3.321E-08	2.817E-08	5.264E-09
dipped	503-49	0.14	1.4	4.410E-08	2.558E-08		
	503-50	0.14	1.5	4.725E-08	2.741E-08		
	503-51	0.13	1.5	4.388E-08	2.545E-08	2.614E-08	1.094E-09
blank	503-53	0.12	2.7	7.290E-08	4.228E-08		
	503-54	0.12	2.8	7.560E-08	4.385E-08		
	503-55	0.12	2.9	7.830E-08	4.541E-08	4.385E-08	1.566E-09
clean	504-01	0.11	4.3	1.064E-07	6.173E-08		
	504-02	0.13	5.5	1.609E-07	9.331E-08		
	504-03	0.12	8.5	2.295E-07	1.331E-07	9.605E-08	3.577E-08
blank	504-04	88.12	2.8	5.552E-08	3.220E-08		
	504-05	89.67	2.8	5.649E-08	3.277E-08		
	504-06	89.78	2.9	5.858E-08	3.398E-08	3.298E-08	9.084E-10
dipped	504-07	0.11	2.9	7.178E-08	4.163E-08		
	504-08	98.47	2.2	4.874E-08	2.827E-08		
	504-09	0.10	2.1	4.725E-08	2.741E-08	3.244E-08	7.974E-09
blank	504-11	0.10		0.000E+00	0.000E+00		
	504-12	0.10	3.0	6.750E-08	3.915E-08		
	504-13	0.10	3.0	6.750E-08	3.915E-08	3.915E-08	0.000E+00

clean	504-15	82.23	2.0	3.700E-08	2.146E-08		
	504-16	79.76	2.8	5.025E-08	2.914E-08		
	504-17	76.84	3.0	5.187E-08	3.008E-08	2.690E-08	4.730E-09
blank	504-18	87.47	3.6	7.085E-08	4.109E-08		
	504-19	86.61	3.2	6.236E-08	3.617E-08		
	504-20	89.95	3.0	6.072E-08	3.522E-08	3.749E-08	3.155E-09
dipped	504-21	87.29	3.0	5.892E-08	3.417E-08		
	504-22	89.80	3.9	7.880E-08	4.570E-08		
	504-23	87.08	3.0	5.878E-08	3.409E-08	3.413E-08	6.681E-09
blank	504-25	92.35	3.8	7.896E-08	4.580E-08		
	504-26	91.91	3.9	8.065E-08	4.678E-08		
	504-27	94.11	3.3	6.988E-08	4.053E-08	4.437E-08	3.361E-09
clean	504-29	91.76	2.3	4.749E-08	2.754E-08		
	504-30	88.92	3.1	6.202E-08	3.597E-08		
	504-31	92.43	3.0	6.239E-08	3.619E-08	3.323E-08	4.930E-09
blank	504-32	87.92	2.7	5.341E-08	3.098E-08		
	504-33	90.92	2.5	5.114E-08	2.966E-08		
	504-34	90.71	2.8	5.715E-08	3.315E-08	3.126E-08	1.759E-09
dipped	504-35	87.83	6.0	1.186E-07	6.877E-08		
	504-36	89.68	5.5	1.110E-07	6.437E-08		
	504-37	91.19	5.1	1.046E-07	6.069E-08	6.461E-08	4.045E-09
blank	504-39	0.11	2.7	6.683E-08	3.876E-08		
	504-40	0.11	2.8	6.930E-08	4.019E-08		
	504-41	0.11	3.0	7.425E-08	4.307E-08	4.067E-08	2.193E-09
clean	504-43	82.22	2.5	4.625E-08	2.682E-08		
	504-44	75.01	4.0	6.751E-08	3.916E-08		
	504-45	74.83	6.1	1.027E-07	5.957E-08	4.185E-08	1.654E-08
blank	504-46	88.22	3.7	7.344E-08	4.260E-08		
	504-47	87.08	3.6	7.053E-08	4.091E-08		
	504-48	87.32	3.1	6.091E-08	3.533E-08	3.961E-08	3.806E-09
dipped	504-49	94.03	3.4	7.193E-08	4.172E-08		
	504-50	99.87	2.5	5.618E-08	3.258E-08		
	504-51	97.56	2.5	5.488E-08	3.183E-08	3.538E-08	5.507E-09
blank	504-53	93.86	2.5	5.280E-08	3.062E-08		
	504-54	92.63	2.9	6.044E-08	3.506E-08		
	504-55	97.09	2.2	4.806E-08	2.787E-08	3.118E-08	3.624E-09
clean	504-57	82.18	3.3	6.102E-08	3.539E-08		
	504-58	84.03	3.0	5.672E-08	3.290E-08	3.414E-08	1.763E-09
	504-59	86.12	2.7	5.232E-08	3.034E-08	3.288E-08	2.523E-09
blank	504-60	0.10	5.7	1.283E-07	7.439E-08		
	504-61	94.58	4.0	8.512E-08	4.937E-08		
	504-62	93.19	3.5	7.339E-08	4.256E-08	5.544E-08	1.676E-08
dipped	504-64	96.22	2.6	5.629E-08	3.265E-08		
	504-65	98.61	2.5	5.547E-08	3.217E-08		
	504-66	98.41	2.7	5.978E-08	3.467E-08	3.316E-08	1.329E-09
blank	504-67	0.10	2.1	4.725E-08	2.741E-08		
	504-68	0.11	2.3	5.693E-08	3.302E-08		

	504-69	0.10	2.5	5.625E-08	3.263E-08	3.102E-08	3.133E-09
clean	504-71	75.83	11.9	2.030E-07	1.178E-07		
	504-72	74.11	6.2	1.034E-07	5.996E-08		
	504-73	75.56	6.3	1.071E-07	6.212E-08	7.995E-08	3.276E-08
blank	504-74	91.12	3.2	6.561E-08	3.805E-08		
	504-75	91.29	4.0	8.216E-08	4.765E-08		
	504-76	88.83	3.8	7.595E-08	4.405E-08	4.325E-08	4.850E-09
dipped	504-77	95.66	4.0	8.609E-08	4.993E-08		
	504-78	93.43		0.000E+00	0.000E+00		
	504-79	94.01	3.1	6.557E-08	3.803E-08	4.398E-08	8.417E-09
blank	504-81	89.08	3.4	6.815E-08	3.952E-08		
	504-82	88.85	3.0	5.997E-08	3.478E-08		
	504-83	88.37	3.1	6.164E-08	3.575E-08	3.669E-08	2.505E-09
clean	505-01	85.20	11.5	2.205E-07	1.279E-07		
	505-02	85.21	10.4	1.994E-07	1.156E-07		
	505-03	84.02	13.8	2.609E-07	1.513E-07	1.316E-07	1.812E-08
blank	505-04	92.27	3.4	7.059E-08	4.094E-08		
	505-05	92.17	3.5	7.258E-08	4.210E-08		
	505-06	93.76	3.5	7.384E-08	4.282E-08	4.195E-08	9.506E-10
dipped	505-07	77.88	1.8	3.154E-08	1.829E-08		
	505-08	88.69	2.1	4.191E-08	2.431E-08		
	505-09	88.64	2.5	4.986E-08	2.892E-08	2.384E-08	5.328E-09
blank	505-11	95.24	2.0	4.286E-08	2.486E-08		
	505-12	94.11	2.1	4.447E-08	2.579E-08		
	505-13	92.86	2.1	4.388E-08	2.545E-08	2.562E-08	2.422E-10
clean	505-15	0.12	2.5	6.750E-08	3.915E-08		
	505-16	0.11	2.0	4.950E-08	2.871E-08		
	505-17	0.11	2.5	6.188E-08	3.589E-08	3.752E-08	2.307E-09
blank	505-18	0.10	3.4	7.650E-08	4.437E-08		
	505-19	0.11	3.3	8.168E-08	4.737E-08		
	505-20	0.10	3.5	7.875E-08	4.568E-08	4.581E-08	1.505E-09
dipped	505-21	0.11	2.5	6.188E-08	3.589E-08		
	505-22	0.10	3.0	6.750E-08	3.915E-08		
	505-23	0.10	3.3	7.425E-08	4.307E-08	3.948E-08	3.594E-09
blank	505-25	0.12	2.5	6.863E-08	3.980E-08		
	505-26	0.12	2.6	7.020E-08	4.072E-08		
	505-27	0.12	2.5	6.750E-08	3.915E-08	3.989E-08	7.866E-10
clean	505-29	89.14	2.0	4.011E-08	2.327E-08		
	505-30	89.08	2.2	4.409E-08	2.557E-08		
	505-31	88.77	2.0	3.995E-08	2.317E-08	2.400E-08	1.362E-09
blank	505-32	88.64	2.8	5.584E-08	3.239E-08		
	505-33	92.27	2.3	4.775E-08	2.769E-08		
	505-34	91.88	3.0	6.202E-08	3.597E-08	3.202E-08	4.151E-09
dipped	505-35	96.36	2.8	6.071E-08	3.521E-08		
	505-36	0.11		0.000E+00	0.000E+00		
	505-37	0.11	2.2	5.445E-08	3.158E-08	3.340E-08	2.566E-09
blank	505-39	98.52	2.5	5.542E-08	3.214E-08		

| 505-40 | 97.04 | 2.0 | 4.367E-08 | 2.533E-08 | | |
| 505-41 | 93.20 | 2.0 | 4.194E-08 | 2.433E-08 | 2.726E-08 | 4.253E-09 |

Bibliography

1. "Biological Warfare." N. pag, http://en.wikipedia.org/wiki/Germ_warfare.

2. Hawley, Robert J., and Edward M. Eitzen Jr. "Biological Weapons – A Primer for Microbiologists," *Annual Review of Microbiology*, 55: 235-53 (2001).

3. "Smallpox," n. pag. http://en.wikipedia.org/wiki/Small_pox.

4. Higgins, James A., Mary Cooper, Linda Schroeder-Tucker, Scott Black, David Miller, Jeffrey S. Karns, Erlynn Manthey, Roger Breeze, and Michael L Perdue. "A Field Investigation of *Bacillus anthracis* Contamination of U.S. Department Buildings of Agriculture and Other Washington, D.C., Buildings during the Anthrax Attack of October 2001," *Applied and Environmental Microbiology*, 69: 593-599 (2003).

5. "2001 Anthrax Attacks," n. pag. http://en.wikipedia.org/wiki/2001_anthrax_attack.

6. Dubroff, Rich. "Postal Facility Undergoes Anthrax Cleanup," n. pag. http://cnn.com/2002/US/South/12/15/anthrax.decon/index.html

7. Beeching, Nicholas J., Davind A. B. Dance, Alastair R. O. Miller, and Robert C. Spencer. "Biological Warfare and Bioterrorism," *British Medical Journal*, 324: 336-39 (2002).

8. Broussard, Larry A., "Biological Agents: Weapons of Warfare and Bioterrorism." *Molecular Diagnosis*, 6: 323-33 (2001).

9. Atlas, Ronald M. "Bioterrorism: From Threat to Reality," *Annual Review of Microbiology*, 56:167-185 (2002).

10. Cieslak, Theodore J. and Edward M. Eitzen, Jr. "Clinical and Epidemiologic Principles of Anthrax," *Emerging Infectious Diseases*, 5: 552-555 (1999).

11. Collier, John R., and John A. T. Young. "Anthrax Toxin," *Annual Review of Cell and Developmental Biology*, 19: 45-70 (2003).

12. Iqbal, Shahzi S., Michael W. Mayo, John G. Bruno, Burt V. Bronk, Carl A. Batt, and James P. Chambers. "A Review of Molecular Recognition Technologies for Detection of Biological Threat Agents," *Biosensors & Bioelectronics*, 15: 549-578 (2000).

13. "Aptamer," n. pag. http://aptamer.icmb.utexas.edu.

14. Hermann, Thomas and Dinshaw J. Patel. "Adaptive Recognition by Nucleic Acid Aptamers," *Science*, 287: 820-825 (2000).

15. Luzi, E., S. Minunni, S. Tombelli, and M. Mascini. "New Trends in Affinity Sensing: Aptamers for Ligand Binding," *Trends in Analytical Chemistry*, 22: 810-818 (2003).

16. McCauley, Thomas G., Nobuko Hamaguchi, and Martin Stanton. "Aptamer-Based Biosensor Arrays for Detection and Quantification of Biological Macromolecules," *Analytical Chemistry*, 319: 244-150 (2003).

17. Savran, Cagri A., Scott M. Knudsen, Andrew D. Ellington, and Scott R. Manalis. "Micromechanical Detection of Proteins Using Aptamer-Based Receptor Molecules," *Analytical Chemistry*, 76: 3194-3198 (2004).

18. Liss, Michael, Birgit Petersen, Hans Wolf, and Elke Prohaska. "An Aptamer-Based Quartz Crystal Protein Biosensor," *Analytical Chemistry*, 74: 4488-4495 (2002).

19. Jiang, Yaxin, Chuanfeng Zhu, Liansheng Ling, Lijun Wan, Xiaohong Fang, and Chunli Bai. "Specific Aptamer-Protein Interaction Studied by Atomic Force Microscopy," *Analytical Chemistry*, 75: 2122-2116 (2003).

20. Piganeau, Nicolas and Renée Schroeder. "Aptamer Structures: A Preview into Regulatory Pathways?" *Chemistry and Biology*, 10: 103-104 (2003).

21. Merino, Edward J. and Kevin M. Weeks. "Fluorogenic Resolution of Ligand Binding by a Nucleic Acid Aptamer," *Journal of American Chemical Society*, 125: 12370-12371 (2003).

22. Dieckman, Thorsten, Samuel E. Butcher, Mandana Sassanfar, Jack W. Szostak, and Juli Feigon. "Mutant ATP-binding RNA Aptamers Reveal the Structural Basis for Ligand Binding," *Journal of Molecular Biology*, 273: 467-478 (1997).

23. "ATP molecule," n. pag. http://en.wikipedia.org/wiki/Adenosine_triphosphate.

24. Nix Jay, Django Sussman, and Charles Wilson. "The 1.3 Å Crystal Structure of a Biotin-binding Pseudoknot and the Basis for RNA Molecular Recognition," *Journal of Molecular Biology*, 296: 1235-1244 (2000).

25. Patel, Dinshaw J, Asif K. Suri, Feng Jiang, Licong Jiang, Pei Fan, R. Ajay Kumar, and Lylvie Nonin. "Structure, Recognition and Adaptive Binding in RNA Aptamer Complexes," *Journal of Molecular Biology*, 272: 645-664 (1997).

26. "AMP molecule," n. pag. http://www.chemfinder.com.

27. "Streptomycin molecule," n. pag. http://www.chemfinder.com.

28. Maier, Raina M., Ian L. Pepper, and Charles P. Gerba. *Environmental Microbiology*. San Diego: Academic Press, 2000.

29. Mock, Michèle and Agnès Fouet. "Anthrax," *Annual Review of Microbiology*, 55: 647-71 (2001).

30. Joklik, Wolfgang K., and Hilda P. Willett. *Zinsser Microbiology*, New York: Appleton-Century-Crofts, 1976.

31. Zollock, Ruth. Characterization of the Surface Morphology of Bacillus Spores by Atomic Force Microscopy. AFIT/GEE/ENV/02M-17. School of Systems and Engineering Management, Air Force Institute of Technology (AU), Wright-Patterson AFB, OH, March 2002 (ADA400732).

32. "Peptidoglycan," n. pag. http://en.wikipedia.org/wiki/Peptidoglycan.

33. Bozue, Joel A., Narayanan Parthasarathy, Lawrence R. Phillips, Christopher K. Cote, Patricia F. Fellows, Itai Mendelson, Avigdor Shafferman, and Arthur M. Friedlander. "Construction of a Rhamnose Mutation in *Bacillus anthracis* Affects Adherance to Macrophages but Not Virulence in Guinea Pigs, *Microbial Pathogenesis*, 38:1-12 (2005).

34. Helgason, Erlendur, Ole Andreas Økstad, Dominique A. Caugant, Henning A. Johansen, Agnes Fouet, Michèle Mock, Ida Hegna, and Anne-Britt Kolsto. "*Bacillus anthracis*, *Bacillus cereus*, and *Bacillus thuringiensis* – One Species on the Basis of Genetic Evidence," *Applied Environmental Microbiology*, 66: 2627-30 (2000).

35. Fox, Alvin, George C. Stewart, Lashanda N. Waller, Karen F. Fox, William M. Harley, and Robert L. Price. "Carbohydrates and Glycoproteins of *Bacillus anthracis* and related bacilli: targets for biodetection," *Journal of Microbiological Methods*, 54: 143-152 (2003).

36. "L-Fucose," n. pag. http://www.aw-bc.com/mathews/ch16/fucose.htm.

37. Forbes, Betty A., Daniel F. Sahm, and Alice S. Weissfeld. *Bailey and Scott's Diagnostic Microbiology*, St. Louis, MO: Mosby, 2002.

38 *Bacillus anthracis* and Anthrax. n. pag., http://textbookofbacteriology.net/Anthrax.html.

39 Brock, Thomas D., Michael T Madigan, John M. Martinko, and Jack Park. *Biology of Microorganisms*, Englewood Cliffs, NJ: Prentice Hall, 1994.

40. Yu, Meng, Albena Ivanisevic. "Encapsulated Cells: an Atomic Force Microscopy Study," *Biomaterials*, 25: 3655-62 (2004).

41. Dufrêne, Yves F., Christophe J. P. Boonaert, Henry C. van der Mei, Henk J. Busscher, and Paul F. Rouxhet. "Probing Molecular Interactions and Mechanical Properties of Microbial Cell Surfaces by Atomic Force Microscopy," *Ultramicroscopy*, 86: 113-20 (2001).

42. Bowen, Richard W., Robert W. Lovett, and Chris J. Wright. "Direct Quantification of *Aspergillus niger* Spore Adhesion to Mica in Air Using an Atomic Force Microscope," *Colloids and Surfaces*, 173: 205-210 (2000).

43. Bruno, John G. and Johnathan Kiel. "In Vitro Selection of DNA Aptamers to Anthrax Spores with Electrochemiluminescence Detection," *Biosensors & Bioelectronics*, 14: 457-464 (1999).

44. *MultiMode™ Scanning Probe Microscope Instruction Manual*, Santa Barbara, CA: Digital Instruments (1996).

45. Fisher Scientific Company. *Protocol Stabilized Gram Stain Set.*

REPORT DOCUMENTATION PAGE

1. REPORT DATE (DD-MM-YYYY) 13-06-2005	2. REPORT TYPE **Master's Thesis**	3. DATES COVERED (From – To) Jun 2004 – May 2005

4. TITLE AND SUBTITLE

Detection of *Bacillus* Spores by Aptamer Selectivity Using Atomic Force Microscopy

5a. CONTRACT NUMBER

5b. GRANT NUMBER

5c. PROGRAM ELEMENT NUMBER

6. AUTHOR(S)

Houtkooper, Nina, M., Captain, USAF

5d. PROJECT NUMBER
If funded, enter ENR #

5e. TASK NUMBER

5f. WORK UNIT NUMBER

7. PERFORMING ORGANIZATION NAMES(S) AND ADDRESS(S)
Air Force Institute of Technology
Graduate School of Engineering and Management (AFIT/EN)
2950 Hobson Way
WPAFB OH 45433-7765

8. PERFORMING ORGANIZATION REPORT NUMBER

AFIT/GAP/ENP/05-03

9. SPONSORING/MONITORING AGENCY NAME(S) AND ADDRESS(ES)
AFRL/HEPC
Attn: Dr. Eric A. Holwitt
2486 Gillingham Dr, BLDG 175E
Brooks City Base, TX 78235   DSN: 240-1192

10. SPONSOR/MONITOR'S ACRONYM(S)

11. SPONSOR/MONITOR'S REPORT NUMBER(S)

12. DISTRIBUTION/AVAILABILITY STATEMENT
APPROVED FOR PUBLIC RELEASE; DISTRIBUTION UNLIMITED.

13. SUPPLEMENTARY NOTES

14. ABSTRACT
The anthrax attack of Oct 2001 demonstrates the need for a rapid detector for spores of *Bacillus anthracis* (BA). Current technology requires cultures of BA to be grown for 24 hours. Using aptamers, a type of nucleic acid ligand selective for a target molecule, to select BA spores for measurement without culturing is a possible solution for quicker detection. An aptamer having a specially selected structure is expected to selectively bind to the surface of its target spore, separating it from other material. An atomic force microscopy (AFM) method was developed to test this selectivity. Aptamers having structure selected to recognize BA were attached to a silicon nitride AFM probe, which was put in contact with spores of *Bacillus anthracis* Sterne strain or *B. thuringiensis* var. kurstaki (BT). Using the AFM in contact mode, the adhesion force between the aptamer and the spores was measured. This research compared the difference in adhesion forces of a clean probe and a probe treated with these aptamers for both BA spores and BT spores to determine whether the enhanced selectivity of aptamers for BA compared with BT could be directly measured.

15. SUBJECT TERMS
Bacillus, *Bacillus anthracis*, Anthrax, *Bacillus thuringiensis*, spores, aptamers, atomic force microscopy

16. SECURITY CLASSIFICATION OF: U			17. LIMITATION OF ABSTRACT	18. NUMBER OF PAGES	19a. NAME OF RESPONSIBLE PERSON Larry W. Burggraf, ENP
REPORT U	ABSTRACT U	c. THIS PAGE U	UU	87	19b. TELEPHONE NUMBER (Include area code) (937) 255-3636, ext 4507; e-mail: Larry.Burggraf@afit.edu